TECHNICAL MEMORANDUM

770

An evaluation of radiative transfer modelling errors in AMSU-A data

Cristina Lupu, Alan Geer, Niels Bormann and Stephen English

Research Department

August 2016

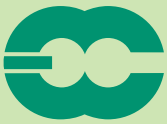

European Centre for Medium-Range Weather Forecasts
Europäisches Zentrum für mittelfristige Wettervorhersage
Centre européen pour les prévisions météorologiques à moyen terme

Series: ECMWF Technical Memoranda

A full list of ECMWF Publications can be found on our web site under:
http://www.ecmwf.int/en/research/publications

Contact: library@ecmwf.int

European Centre for Medium-Range Weather Forecasts
Shinfield Park, Reading, RG2 9AX, England

Abstract

Systematic biases are observed between AMSU-A observations and simulations from numerical weather prediction models. They are not just a simple offset but instead exhibit a complex global pattern that appears to be related to the temperature profile. These errors could arise from inaccuracies in the radiative transfer model calculations used to simulate AMSU-A radiances from the model fields, from poorly-characterised aspects of the instrument calibration and spectral response function, or from errors in the forecast model state. Two hypotheses to explain and model the biases in AMSU-A are examined in this work. First, the optical depth of the atmosphere may not be sufficiently well-modelled due to unknown systematic errors in the the radiative transfer model. In order to correct this, an empirically-derived multiplicative scaling can be applied to the simulated optical depths (the so-called γ-correction). Second, the reported locations of AMSU-A passbands may be incorrect, with empirically-derived corrections of up to 68 MHz having been suggested. Corrections to the radiative transfer modelling based on these hypotheses have been tested in the ECMWF data assimilation system and evaluated in terms of first-guess departure fits to independent observations and forecast scores, or in terms of residual biases to the AMSU-A data itself.

When AMSU-A channels 6–8 are simulated using corrected channel central frequencies (passband shifts), there are generally clear improvements in the fit between model and observations in these channels. However some degraded fits between model and observations are noticed for upper-tropospheric and lower-stratospheric AMSU-A channels, as well as for independent observations (e.g., ATMS, IASI). This also translates into medium-range forecast score degradations. The γ-corrections generally do the best in terms of fits to AMSU-A channels 6–8 and unlike the passband shifts they do not degrade the fit between model and observations in upper-tropospheric and lower-stratospheric AMSU-A channels and the short-range forecasts in the lower stratosphere for independent observations. However, neither of the available hypotheses can fully explain the origin of the systematic biases between models and AMSU-A observations, and both show some degradations in medium-range forecasts.

1 Introduction

Systematic biases relative to numerical weather-prediction (NWP) models are often observed in Advanced Microwave Sounding Unit-A (AMSU-A) channels sensing in the 50-58 GHz range. These biases could arise from inaccuracies in the radiative transfer model (RTTOV; Saunders *et al.*, 1999; Matricardi *et al.*, 2004) calculations that are used to simulate radiance observations from the model state (e.g., errors in the spectroscopic database, continuum effects, line mixing), or from the instrument itself (e.g. poor calibration or characterization). They can also be due to the NWP models which can have consistent biases in their representation of the atmosphere (Dee, 2005). The adequate treatment of systematic errors that exist in the assimilation of satellite radiances is essential to the successful use of these observations in NWP.

Watts and McNally (2004) suggested that the observed AMSU-A bias and its air-mass dependent variation could be explained through systematic errors in the radiative transfer model. They showed how this can be modelled with the so-called [γ, δ] method, which scales the optical depths in the radiative transfer model with a channel-specific γ, and can model the remaining bias with a constant δ. Both γ and δ are assumed to be global constants which depend only on the satellite and the channel. The γ scalings are currently applied at ECMWF for AMSU-A channels 5 to 8 on some of the platforms (i.e., NOAA-15, -16, -18, Aqua) to reduce the magnitude of the global mean biases as well as the air mass dependent biases. More recently, a study by Lu and Bell (2014) suggested that tropospheric AMSU-A sounding channels 6 (54.40 GHz), 7 (54.94 GHz) and 8 (55.50 GHz) on many satellites exhibit significant shifts and drifts relative to nominal pass band center frequencies, that will be manifested as air mass dependent bias as

well as cross scan bias (Peubey and Bell, 2014). The passband shift is a physical mechanism hypothesised by Lu and Bell (2014) to explain much of the biases observed in AMSU-A channels 6 to 8. The effects of pass band shifts are expected to result in biases similar in geographical form to those resulting from errors in spectroscopic parameters. The current study assesses these two possible approaches to mitigating AMSU-A biases in the ECMWF assimilation system.

Where the source of biases between observations and NWP analysis fields is not well-understood, NWP centres rely on bias correction. ECMWF uses a variational bias correction scheme (VarBC; Dee, 2005; Auligné *et al.*, 2007). Estimation of the bias parameters for each instrument channel is achieved by including them in the 4D-Var control variable so that the bias estimates are adjusted simultaneously with the atmospheric variables, using all the information available to the analysis. For a given channel, the observed bias depends on the state of the instrument (e.g., scan position) and varies in time (e.g. diurnally or seasonally) and in space, including changes in the air mass and in the underlying surface (e.g. land, sea or ice). VarBC bias corrections are applied to all radiance sensors assimilated at ECMWF, including AMSU-A, and they include a scan bias and an air mass bias components. Hence, instead of using γ corrections or passband shifts, we could just allow VarBC to adaptively correct all the AMSU-A bias, assuming that the bias maps well onto the available predictors.

A γ-correction or a bandpass shift are not the only hypotheses that have been suggested to explain observed biases. Intercalibration of AMSU-As using simultaneous nadir overpass (SNO) has characterised biases in terms of constant or drifting global radiance offset (e.g. a fixed offset calibration error), solar heating of the instrument, nonlinear calibration effects, and a passband shift from prelaunch measurements in certain satellite channels (i.e., AMSU-A channel 6 on NOAA-15; Zou and Wang, 2011). An advantage of testing the γ-correction and bandpass shift with an actively updated VarBC is that any additional error sources such as these should be removed by the bias correction.

In practice the Watts and McNally (2004) or Lu and Bell (2014) corrections are achieved through the use of different coefficient tables in RTTOV. Hence this work is a follow-on effort to the revision of microwave coefficient files used with RTTOV-11 in the ECMWF's forecasting system (Lupu and Geer, 2015; Lupu *et al.*, 2015). The memorandum is organized as follows. Section 2 reviews the main characteristics of the AMSU-A instrument. The standard RTTOV-11 regression coefficient files are outlined in Section 3. This is followed by a brief description of ECMWF's current and revised γ-values in AMSU-A coefficient files, alongside with the shifted passband AMSU-A coefficient files. Data assimilation experiments have been carried out in Section 4 and the impact of revised-γ values and of shifted AMSU-A coefficient files is assessed by comparing their performance on the ECMWF analyses and forecast with respect to the standard AMSU-A coefficient files. Conclusions are provided in Section 5.

2 AMSU-A instrument

AMSU-A is a cross-track microwave instrument mainly designed for atmospheric temperature sounding on board several polar orbiting satellites such as, the National Oceanic and Atmospheric Administration (NOAA) satellites, the National Aeronautics and Space Administration (NASA) Aqua mission and the European Organisation for the Exploitation of Meteorological Satellites (EUMETSAT) Metop-A/B missions. AMSU-A includes 12 sounding channels (channels 3-14) located near the oxygen absorption band (50-58 GHz) which allow atmospheric temperature sensing from the surface to about 1 hPa and 3 imaging channels at 23.8 GHz (channel 1), 31.4 GHz (channel 2) and 89 GHz (channel 15) sensitive to water vapour, cloud and precipitation. Table 1 summarizes the general specifications of AMSU-A channels and their approximate peak level.

Table 1: Channel specifications of AMSU-A. Polarisation at nadir is either vertical (v) or horizontal (h) but varies across the scan.

Channel Number	Frequency [GHz]	Polarisation (nadir)	Peak level (nadir) Pressure [hPa]	Peak level (nadir) Altitude [km]
1	23.8	v	1013.25	0
2	31.4	v	1013.25	0
3	50.3	v	1013.25	0
4	52.8	v	900	1
5	53.596+/-0.115	h	700	3
6	54.4	h	400	8
7	54.94	v	250	11
8	55.5	h	150	14
9	57.29	h	90	17
10	57.29+/- 0.217	h	50	20
11	57.29+/- 0.3222+/- 0.048	h	25	25
12	57.29+/- 0.3222+/- 0.022	h	10	31
13	57.29+/- 0.3222+/- 0.010	h	5	37
14	57.29+/- 0.3222+/- 0.0045	h	2.5	41
15	89	v	0.01	45

Table 2: Equatorial crossing times and the assimilated channels for each AMSU-A instrument as of 1st July 2013.

Satellite	Equatorial crossing times	Channels assimilated at ECMWF
NOAA-15	16:43	5 and 7 to 13
NOAA-16	8:36	5 to 7 and 10 to 14
NOAA-18	14:57	5 to 14
NOAA-19	13:33	5, 6 and 9 to 14
Aqua	13:37	6 and 8 to 14
MetOp-A	9:30	5, 6 and 8 to 14
MetOp-B	9:30	5 to 14

Over the years, microwave radiance observations from up to seven AMSU-A instruments (i.e., NOAA-15, -16, -18, 19, Aqua, MetOp-A and -B) have been assimilated in clear-sky conditions in ECMWF operational 12-h 4D-Var data assimilation system (Rabier *et al.*, 2000). AMSU-A observations provide a very good global coverage and contribute substantially to today's forecast skill (Bormann *et al.*, 2011; Cardinali, 2009). Note that it is the near-real-time available level 1b radiances that are being assimilated, after an antenna patern correction has been applied.

AMSU-A temperature sounding channels assimilated in this study are summarised in Table 2. Although many AMSU-A channels are assimilated, some have been excluded from the ECMWF data assimilation system when the noise has exceeded specifications. As an example, channel 7 on NOAA-19, Aqua and MetOp-A and channel 8 on NOAA-16 and NOAA-19 were not available during the testing period used here (i.e., July 2013 to February 2014). Moreover, after years of being blacklisted, AMSU-A channel 8 on NOAA-16 returned to operational use at ECMWF on June 2013 and was used up to June 2014, when following a spacecraft anomaly the NOAA-16 satellite was decommissioned.

The VarBC bias correction for AMSU-A attempts to correct scan bias through a third-order polynomial regression in the scan angle. The air-mass bias is latitudinally dependent and is expressed as a linear combination of state-dependent predictors. For AMSU-A a global constant offset and a set of four predictors

derived from the model background are used at ECMWF: 1000-300 hPa, 200-50 hPa, 10-1 hPa and 50-5 hPa layer thicknesses (Harris and Kelly, 2001; Bormann and Bauer, 2010). The highest-peaking AMSU-A channel 14 is currently assimilated without a bias correction and successfully anchors the stratospheric analysis (McNally, 2007; Di Tomaso and Bormann, 2011). Further details on the assimilation of AMSU-A data at ECMWF can be found in Di Tomaso and Bormann (2011) and Lawrence and Bormann (2015).

3 AMSU-A regression coefficient files

3.1 Standard RTTOV-11 files

RTTOV-11 regression coefficient files for AMSU-A are based on 54 fixed vertical pressure levels and the AMSUTRAN line-by-line model, which utilizes the 1989 version of the Liebe Millimeter-wave Propagation Model (MPM-89) for the water-vapour lines (Liebe, 1989) and the 1993 version of the Liebe MPM-93 model with coefficients from the Liebe MPM-92 model for the oxygen (O_2) and nitrogen (N_2) lines (Liebe *et al.*, 1993, 1992). The AMSU-A coefficient files use the optical depth predictors version 7 (Saunders *et al.*, 1999), which has 10 predictors for mixed gases, 15 for water vapour and 11 for ozone and are calculated from the 83 profile training set described in Matricardi (2008). The standard RTTOV coefficient files do not apply any γ-factor transmittance corrections.

In what follows, we will introduce two sets of modified AMSU-A coefficient files for use with RTTOV-11: the first one uses a γ-factor transmittance correction for AMSU-A channels 5 to 8, whereas the second one uses modified passband shifts of the central frequency for AMSU-A channels 6 to 8.

3.2 The γ-correction

A modification to the radiative transfer model was introduced at ECMWF to account for biases arising from errors in the optical depth calculations and hence the weighting function for lower tropospheric AMSU-A observations (Watts and McNally, 2004). To do that AMSU-A coefficient files were updated for use at ECMWF to include empirical γ-factor transmittance corrections. Biases in the optical depth calculation addressed by gamma may arise, for instance, from deficiencies in the spectroscopy, the modelling of line characteristics and coupling between spectral lines, or instrument-specific deviations from the assumed passband-characteristics.

3.2.1 ECMWF operational γ-corrections

The ECMWF operational γ-corrections are shown in Table 3, and are of the order of a few percentages on NOAA-15, -16, -18 and Aqua. For AMSU-A instruments that have been added later to the ECMWF operational system (i.e., MetOp-A, MetOp-B and NOAA-19) no γ-corrections have been derived and no γ-corrections are currently applied (i.e., $\gamma = 1$).

Di Tomaso and Bormann (2011) estimated the value of γ for AMSU-A channels 5 to 8 on two of the recent platforms (i.e., NOAA-19 and MetOp-A) and re-calculated the γ-corrections for AMSU-A on NOAA-15, -18 and Aqua. However, at the time of their study new RTTOV-11 coefficient files were being planned for release, so the AMSU-A coefficient files were left unchanged in the normal ECMWF operational configuration. This study does not perform any experiments with the original γ-corrections or those of Di Tomaso and Bormann (2011). The operational corrections are presented because they were

Table 3: ECMWF operational AMSU-A γ-corrections.

Satellite Channel	NOAA-15	NOAA-16	NOAA-18	Aqua	MetOp-A	MetOp-B	NOAA-19
5	1.050	1.053	1.042	1.050	1.000	1.000	1.000
6	1.050	1.040	1.018	1.039	1.000	1.000	1.000
7	1.034	1.047	1.039	1.045	1.000	1.000	1.000
8	1.040	1.055	1.035	1.046	1.000	1.000	1.000

derived around the years 2004 to 2006 and they can be compared to more recent estimates, which may give an indication of any bias drifts. For testing we will look at a more self-consistent and up-to-date set of corrections.

3.2.2 ECMWF revised γ-corrections

The AMSU-A γ-correction values have been re-estimated, based on ECMWF departures from July and December 2013, using RTTOV-11 and the most recent set of RTTOV-11 microwave coefficient files with 54 vertical levels. For all available AMSU-A channels 5 to 8, γ adjustments to transmittance values have been calculated, by minimizing the geographical variation in the bias against the background. The revised γ-values are listed in Table 4. Boldface entries show AMSU-A channels that are no longer used in the assimilation due to instrument issues, which means that it is no longer possible to estimate revised γ-values. Instead the operational γ-values were kept unchanged in the coefficient files (i.e., AMSU-A channel 6 on NOAA-15, channel 8 on NOAA-16 and channel 7 on Aqua). In a few cases it was possible to take the 2011-based values (Aqua channel 5 and 6, Metop-A channel 8, Di Tomaso and Bormann, 2011). No corrections were available for NOAA-19 channels 7 and 8 and Metop-A channel 7, but these channels are not examined here.

In many cases the revised corrections are similar to the operational ones given in Table 3 for any AMSU-A sensors where gamma correction were applied. However, channels 6 and 7 of NOAA-16 appear to have increased γ-values, while channel 5 on NOAA-15, -18 and Aqua has reduced γ-values compared to the operational values in Table 3. If changes in radiative transfer modelling (such as a different choice of training dataset or different spectroscopy) were affecting the AMSU-A air-mass dependent biases, or if forecast model biases have changed since the γ-corrections were last derived, it might have been expected that corrections for all instruments would have changed in similar ways. The change in channel 5 corrections is consistent with these hypotheses but the large changes to NOAA-16 are not. The NOAA-16 channel 6 and 7 corrections are at least twice as large as those for the other instruments where recent corrections could be derived (e.g. 1.060 and 1.088 compared to 1.017 – 1.030 and 1.029 – 1.034 in channels 6 and 7 respectively). The most likely explanation is that NOAA-16 has a calibration drift or instrument characterisation error that has got worse through its lifetime, as also observed by Zou and Wang (2011) and Lu and Bell (2014).

3.3 Accounting for a passband shifts in AMSU-A coefficient files

Lu and Bell (2014) proposed a precise physical explanation for the air mass biasses addressed by the [γ, δ] method, suggesting that most of the air mass biases are likely due to shifts, drifts and uncertainties in the AMSU-A channel center frequencies. In their study, the variance of the first guess departures for AMSU-A observations is minimized by iteratively adjusting the passband center frequency for each

Table 4: ECMWF revised AMSU-A γ-corrections.

Satellite Channel	NOAA-15	NOAA-16	NOAA-18	Aqua	MetOp-A	MetOp-B	NOAA-19
5	1.025	1.047	1.010	1.031	1.010	1.015	1.020
6	**1.050**	1.060	1.020	1.030	1.017	1.012	1.021
7	1.030	1.088	1.034	**1.045**	**N/A**	1.029	**N/A**
8	1.038	**1.055**	1.038	1.038	1.044	1.041	**N/A**

AMSU-A channel. Where a shift in the assumed centre frequency results in a significant improvement (i.e., of 10% or more reduction in the standard deviation of the first guess departures) the estimated shift is assumed to be real. The conclusions of Lu and Bell (2014) analysis of AMSU-A channel frequency shift can be summarized as follows:

- The lower tropospheric AMSU-A channels 6 to 8 show large shifts relative to the nominal centre frequencies. This was attributed to error occurring in the local oscillator, an electronic device that determines the central channel frequency value. Although the shifts take generally the form of a constant offset throughout the life of the satellite, for some channels the local oscillator drifts with time (i.e., channel 6 on NOAA-15 and channels 6 to 8 on NOAA-16). The shifts diagnosed for the lower peaking AMSU-A channels 6 to 8 improve the fit between observations and NWP models.
- Although substantial frequency shifts were found in AMSU-A channels 6 to 8, small or near-zero shifts were diagnosed for AMSU-A channels 9 to 14, and this was attributed to the active frequency locking of these channels that appears to stabilize these channels (Peubey *et al.*, 2011).
- The estimated shifts for AMSU-A channels 6 to 8 were relatively insensitive to the choice of NWP model (i.e., ECMWF, Met Office, NCEP and CMA) and to the new set of spectroscopic parameters for the 50-58 GHz oxygen (O_2) absorption band (Tretyakov *et al.*, 2005).
- Not all the estimated shifts for AMSU-A channels 6 to 8 lead to reductions in the standard deviations of the first guess departures of more than 10%. For example, no significance is attributed by Lu and Bell (2014) to the derived shifts for channel 6 on NOAA-18, NOAA-19, MetOp-A and Aqua, for channel 7 on MetOp-A and Aqua and for channel 8 on NOAA-19.
- The analysis of frequency shifts for AMSU-A on MetOp-B and for the lower peaking AMSU-A channel 5 on all platforms was not covered by the study.

Table 5 shows the derived passband shifts for tropospheric AMSU-A sounding channels 6 to 8 estimated using the short-range forecast fields from the ECMWF model, using data from August 2011 (Lu and Bell, 2014). Shifts of tens of MHz (e.g., 10-68 MHz) relative to pre-launch measurements were diagnosed. Channels with significant diagnosed shifts are shown with boldface entries in Table 5. These passband shifts can be incorporated in the pre-computed RTTOV coefficients, leading to a third set of coefficient files that can be tested in the ECMWF system.

In this study passband shifted RTTOV coefficients for Metop-B were not available and so the standard RTTOV-11 coefficients were used for this satellite. Also, all passband shifts values listed in Table 5 have been incorporated in the coefficient files even for those channels for which no significance was attributed to the shifts by Lu and Bell (2014). Furthermore, the temporal drifts in NOAA-15 channel 6 and NOAA-16 channels 6 to 8 were not accounted for; for these channels the shifts diagnosed in 2011 were used.

Table 5: Passband shifts [MHz] for AMSU-A channels 6 to 8, as calculated by Lu and Bell (2014) using data from August 2011.

Channel	NOAA-15	NOAA-16	NOAA-18	NOAA-19	Aqua	MetOp-A
6	**40**	**26**	14	12	18	10
7	**24**	**52**	**30**	**26**	28	36
8	**28**	**68**	**36**	32	**38**	**32**

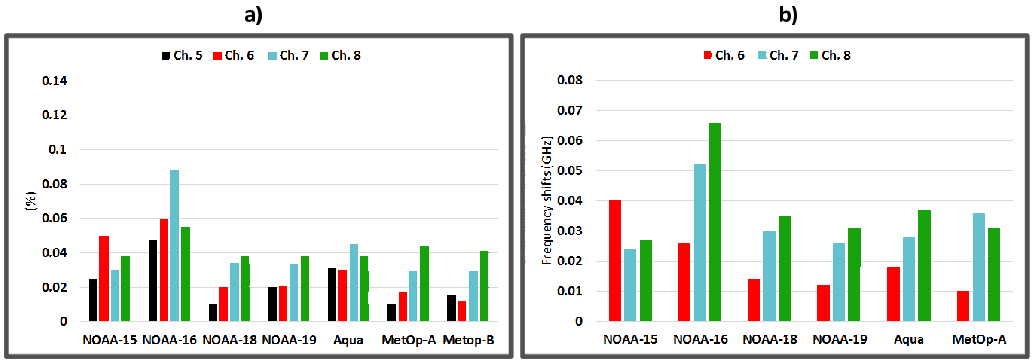

Figure 1: a) Relative change in the absorption coefficient (%) for AMSU-A channels 5-8 on 7 satellites; b) The derived passband shifts (GHz) for AMSU-A channels 6-8 on 6 satellites.

Figure 1 shows graphically the ECMWF revised γ-correction for AMSU-A channels 5-8 and the derived passband shifts for AMSU-A channels 6 to 8. AMSU-A channel 6 on NOAA-15 and AMSU-A channels 6 to 8 on NOAA-16 show the largest corrections, whether expressed in terms of a γ-correction or a shift in the channel center frequency. Other AMSU-A instruments such as NOAA-18, -19, Aqua and MetOp-A require smaller corrections, and the corrections are more similar from one instrument to another. This suggests that the γ-correction and the passband shift are addressing similar air-mass dependent biases, and this will be confirmed later. Further, the similarity of the required corrections, at least excluding channels 6 to 8 on NOAA-16 and NOAA-15 channel 6, leaves open the possibility that some part of these corrections may actually be accounting for some other error, perhaps in the forecast model, or in the calibration and characterisation of every AMSU-A.

3.4 Impact of different AMSU-A coefficient tables on temperature Jacobian

The sensitivity of individual channels in the 50 GHz oxygen band (channels 5 to 14) to different heights is illustrated by their temperature Jacobians, displayed in Fig. 2a for a standard mid-latitude reference profile. Because oxygen is well-mixed, these Jacobians show little variation across the globe (not shown) despite large variations in the temperature profile (Fig. 2b). However, the large global variations in the temperature profile means that any errors in the Jacobians could be manifested differently across the globe, in other words as an air-mass dependent bias.

Temperature Jacobians for AMSU-A channels 6 to 8 on NOAA-16 and NOAA-18 obtained using the three different RTTOV coefficient tables are shown in Figs. 3 and 4 respectively. The largest corrections are being made in NOAA-16 channels 7 and 8 (Fig. 3 panels b and c), where it is clear there is a different

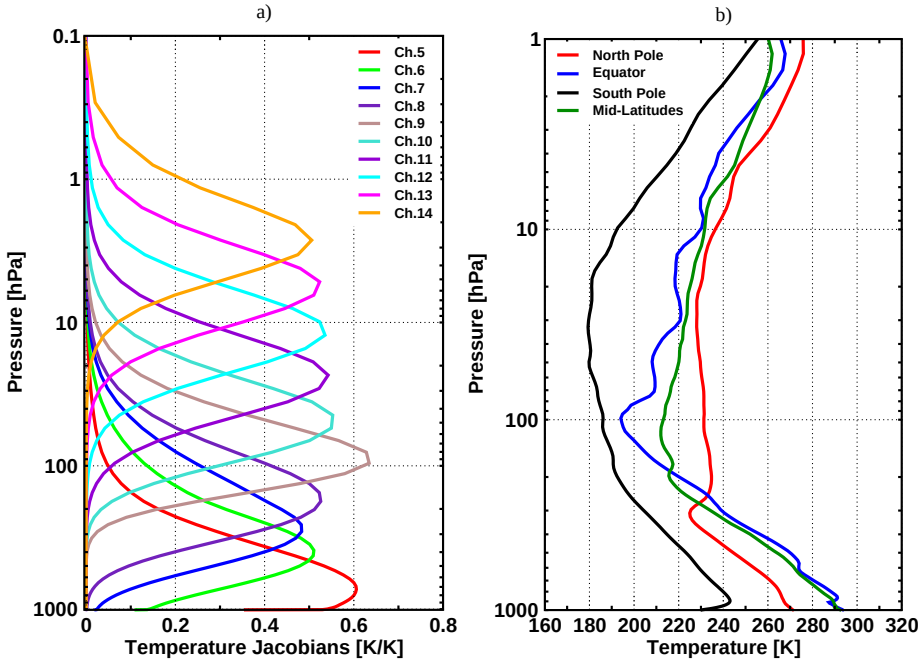

Figure 2: (a) Temperature Jacobians for AMSU-A temperature sounding channels 5 to 14 for a standard mid-latitude reference profile. These Jacobians are normalised by the change in the natural logarithm of pressure for each model level. (b) August 15th 2013 vertical temperature profiles at approximately 45°north or south latitude (mid-latitudes, green line), near the equator (blue line) and near the poles (red and black lines).

response to a γ-correction as compared to a passband shift. A γ-correction greater than one shifts the Jacobian upwards in the atmosphere while keeping its vertical extent mostly unchanged. In contrast, a passband shift tends to broaden the Jacobian and to introduce a stronger sensitivity to the temperature profile between 10 hPa and 60 hPa, in other words a stronger 'stratospheric tail'. This effect on the stratospheric tail does not appear to have been considered in previous work (Zou and Wang, 2011; Lu *et al.*, 2011; Lu and Bell, 2014). These AMSU-A channels are fitted into narrow gaps between stronger absorption lines (e.g. Lu *et al.*, 2011), so shifting the bandpass will include some part of these stronger absorption lines, broadening the weighting function to include higher altitudes. For other satellites with less extreme corrections like NOAA-18 (Fig. 4), the effects are more subtle but still apparent.

4 An assessment of AMSU-A coefficient files in the ECMWF Integrated Forecasting System (IFS)

4.1 Experiments set-up

Assimilation experiments have been performed to assess the use of either AMSU-A coefficient files with revised γ values or with improved passband centre frequencies. For this evaluation we use as reference the RTTOV-11 standard AMSU-A coefficient files with no additional corrections. Experiments cover an 8 month period (July 2013 to February 2014) and are performed using the full observing system of conventional and satellite observations and the ECMWF's 12-h 4D-Var system model cycle 40r2 of the ECMWF forecasting system. However, the satellite assimilation configuration is that used in model cycle 40r3 (e.g., Lupu *et al.*, 2015). The horizontal resolution is T_L511 (around 40 km) and 137 vertical levels

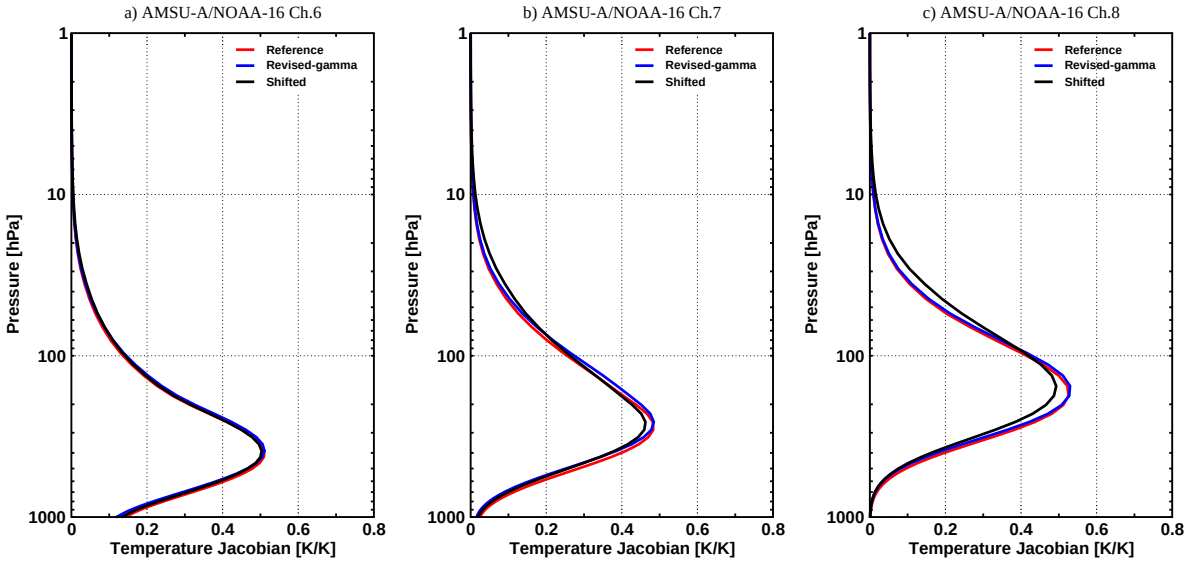

Figure 3: Impact of changes in NOAA-16 coefficient tables on RTTOV-11 simulated AMSU-A weighting functions at near-nadir for a mid-latitudes atmospheric temperature profile: (a) channel 6, (b) channel 7 and (c) channel 8. Temperature Jacobians are normalised by the change in the natural logarithm of pressure for each model level and are shown for a set of three different AMSU-A coefficient files: the standard RTTOV-11 regression coefficient files ('Reference', red line), the ECMWF revised γ-factor AMSU-A coefficient files ('Revised-γ', blue line) and the shifted passband AMSU-A coefficient files ('Shifted', black line).

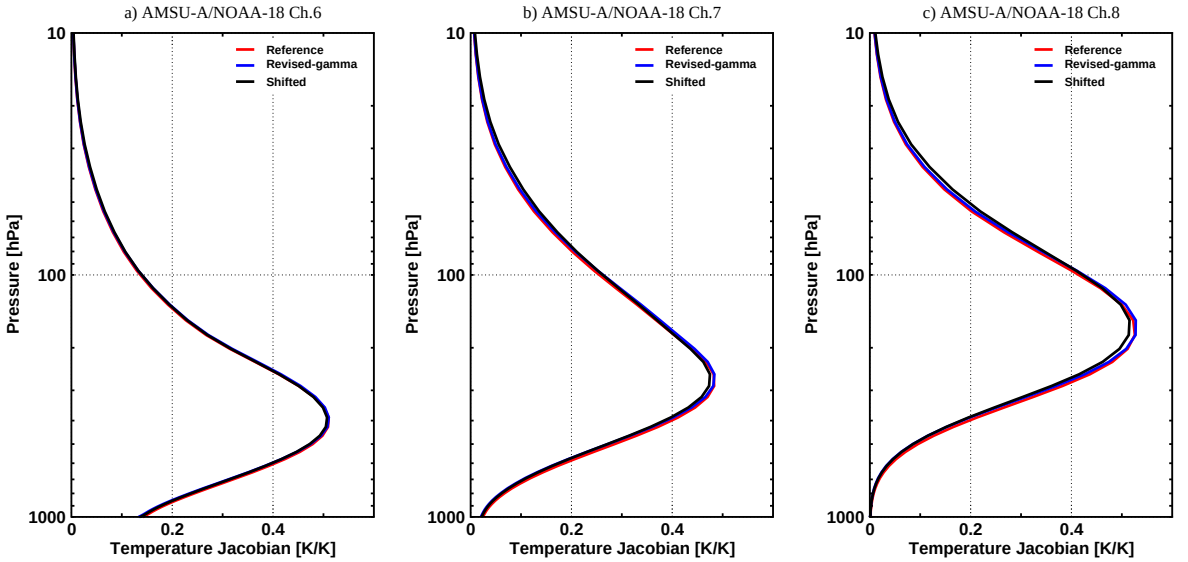

Figure 4: Same as Figure 3 but for AMSU-A on NOAA-18 channels 6 to 8.

with the model top level pressure at 0.01 hPa. Three active assimilation experiments have been run using this configuration, but with different AMSU-A coefficient files as follows:

- **'Reference run'**: Use the RTTOV-11 specific AMSU-A coefficient files, that is $\gamma = 1$ for channels 5 to 8 on all seven platforms (i.e., NOAA-15, -16, -18, -19, Aqua, MetOp-A, -B).

- **'Revised-γ run'**: Use AMSU-A coefficient files with revised γ-values for channels 5 to 8 on all seven platforms (i.e., Table 4).

- **'Shifted run'**: Use AMSU-A coefficient files based on improved passband centre frequencies for channels 6 to 8 on six platforms, but leaving Metop-B coefficients unchanged as the passband shifts were not available (i.e., Table 5).

All experiments were initialized on 1st July 2013 from the ECMWF operational analysis. As well as the atmospheric fields, the initial conditions include the bias coefficients from the operational VarBC file. For AMSU-A, all three experiments use the standard operational VarBC setup described in section 2. A month's spinup has been discarded from the beginning of each experiment to allow bias corrections to adjust to the new bias conditions resulting from the changes in the radiative transfer model.

4.2 AMSU-A biases

Figure 5 shows the spatial pattern of observed minus simulated Metop-A AMSU-A biases in channels 6, 8, 9 and 10, as derived from the 62 assimilation cycles in August 2013 (note that channel 7 is not available on this instrument). The mean of the first-guess (FG) departures has been computed before bias correction, but then the global mean bias has been removed to focus attention on the spatial patterns. Many of the features are common across several channels, for example the relative negative biases over the southern polar regions and relative positive biases over high northern latitudes. These may be linked with broad details of the vertical temperature structure of the atmosphere. For example (e.g., Fig. 2b) in August the polar vortex is established over the south pole, giving a temperature minimum below 190 K at 50hPa and no distinct tropopause, but over the northern high latitudes the lower stratosphere is fairly isothermal above 230 K between the tropopause at 300 hPa up to about 10 hPa (see also Kållberg *et al.* , 2005). Channel 8 has a weighting function peaking at 150 hPa, so its bias pattern could suggest that modelled lower stratospheric temperatures are relatively too warm over the south pole and the tropics, but relatively too cold over high northern latitudes. However, this pattern could also be explained by moving the weighting function to slightly higher altitudes, which would have less effect on simulated brightness temperatures in the northern high latitudes where the lower stratosphere is relatively isothermal, but it would cause a more significant decrease in modelled brightness temperatures in the southern polar vortex and at the tropical tropopause, where atmospheric temperature continues to decrease above 150 hPa.

Figure 6 shows the same channels after variational bias correction. The air-mass dependent biases shown in Figure 5 can be modelled as linear functions of the four geopotential thickness predictors available for AMSU-A, and with these modelled biases removed, there is very little remaining monthly-mean bias in the AMSU-A radiances, neither in the global means or the spatial patterns.

The air-mass dependent biases shown in Figure 5 can also be addressed by the γ-correction method of Watts and McNally (2004) and the passband corrections (Lu and Bell, 2014). Figure 7 shows maps

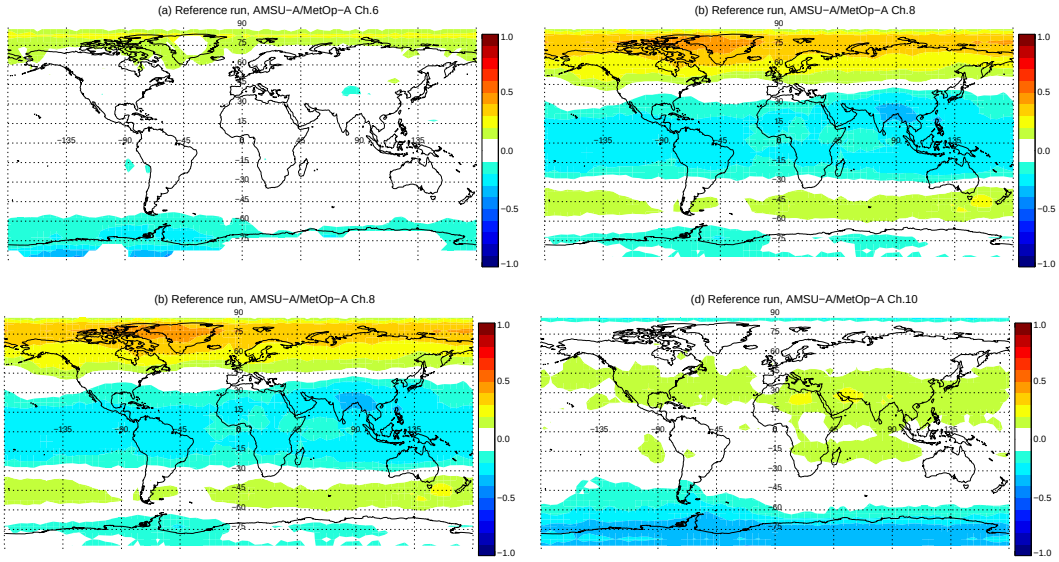

Figure 5: Mean of first-guess departures before bias correction, binned to a 5° latitude-longitude grid, but with the mean bias correction removed for AMSU-A on MetOp-A channels 6, 8, 9 and 10 from the 'Reference run'. The sample is based on the period 1 to 31 August 2013.

of mean FG-departures before bias correction for NOAA-18 AMSU-A channel 7 for August 2013 in the 'Reference run' where γ=1, in the 'Revised-γ run' where a γ=1.039 and in the 'Shifted run' where a shift of 30 MHz from the nominal passband center frequency of 54.94 GHz is used. Both of these corrections would have the broad effect of shifting the channel 7 weighting function slightly higher in the atmosphere. Increasing the peak height of the weighting function broadly lowers the simulated brightness temperature, and as a result both corrections bring the mean of biases in the FG-departure closer to zero. Also, as explained in the context of Figure 2, regional differences in the temperature profile mean that simulated brightness temperatures in tropical and southern polar regions would be lowered more sharply than elsewhere. Hence, these corrections do reduce the latitudinal variation in the FG-departures, although not completely.

After application of the variational bias correction, the FG-departure fields in Figure 8 look fairly similar between the three experiments. This shows that if necessary, VarBC on its own can be used to correct the biases and that the passband shifted coefficients or gamma correction give similar results, at least in this monthly mean view.

Figures 9, 10 and 11 examine the effect of the different coefficient files on AMSU-A channel 7, but considering the instruments on different platforms (NOAA-15, NOAA-18 and MetOp-B) and removing the global mean bias from each figure to concentrate on the air-mass dependent part of the bias. Without a γ-correction or passband shift (Figure 9) the channel 7 biases are quite similar to each other, and also quite similar to those in channel 8 (as shown in Figure 5 for Metop-A). After γ-correction or passband shift, most of this bias is removed, though NOAA-19 and (for γ-corrections) the Metop-B retain slightly more negative departures over the south pole (note that no passband shift information was available for Metop-B). Broadly the same conclusions can be drawn as from the examination of NOAA-18 alone, that both γ-correction and passband shifts are effective at removing the air-mass dependent bias, but VarBC is required to completely suppress the bias, and indeed it is capable of removing the monthly mean bias

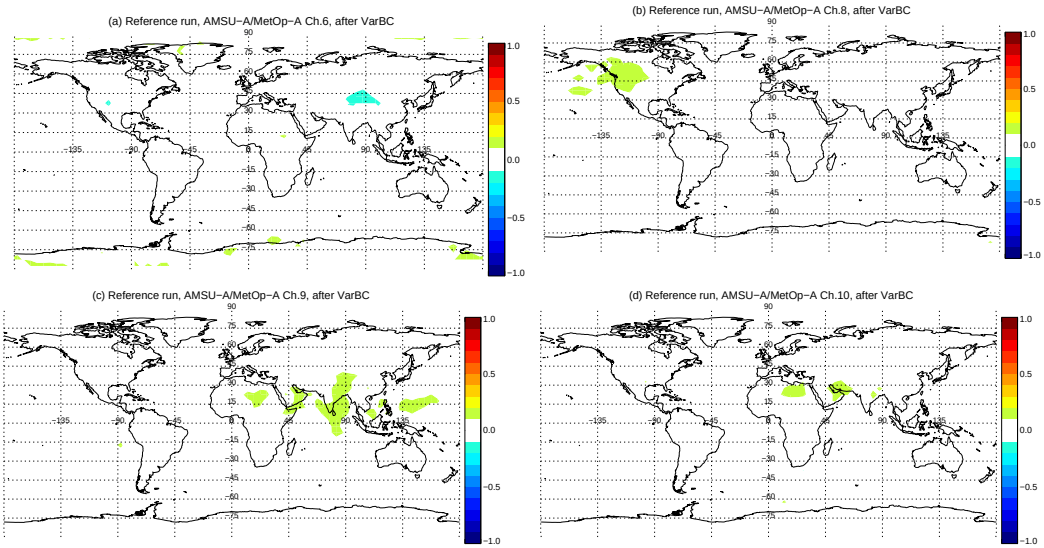

Figure 6: Same as Figure 5 but after bias correction.

on its own.

The γ-correction and passband shifts are also expected to address cross-scan dependent bias that is associated with the relative increase in the height of the weighting functions towards the edge of the swath where zenith angles are highest. Figure 12 shows the variation in the biases for AMSU-A channel 7 on NOAA-18. Mean and standard-deviation of FG-departures were generated from data actively assimilated during August 2013 in all three experiments. It appears that using the γ-correction or the passband shifts in AMSU-A coefficient files improves both the mean and the standard deviation of FG departures before bias correction in AMSU-A on NOAA-18 channel 7 (Figures 12a and 12b). Also for the lower tropospheric channels 5 to 8 we observe less variation in FG-departures from scan edges to nadir as well as a smaller offset from zero (not shown). These are consistent with results shown in Lean *et al.* (2014). After application of the variational bias correction, there is very little difference between the FG-departure statistics (Figure 12c and 12d).

Furthermore, the scan-angle biases of AMSU-A are latitude-dependent, as illustrated in Figures 13 and 14. The tails at the edges of the scanline also vary with latitude. Cross-scan biases reduced when including the γ scaling factor or the passband shift in the radiative transfer calculations. We notice a reduction of spread across latitude bands and the latitudinal biases are closer together on the whole, particularly for channel 8, in both 'Revised-γ' and 'Shifted' runs (not shown). As a result, the variational bias-correction scheme has to do less work to correct the cross-scan bias. The variational bias correction successfully removes biases for all scan-positions on the basis of a third order polynomial in the scan-position. The differences between the three experiments are quite small, thus the reduction in the amplitude across latitude bands still persist in the 'Shifted' run.

We next examine global standard deviations of departures for each of the AMSU-A instruments as well as for all AMSU-A sensors aggregated together.

Figure 15 shows the standard deviation of first guess departures after the bias correction, given as a percentage relative to the 'Reference run' for individual AMSU-A sensors and for all AMSU-A sensors

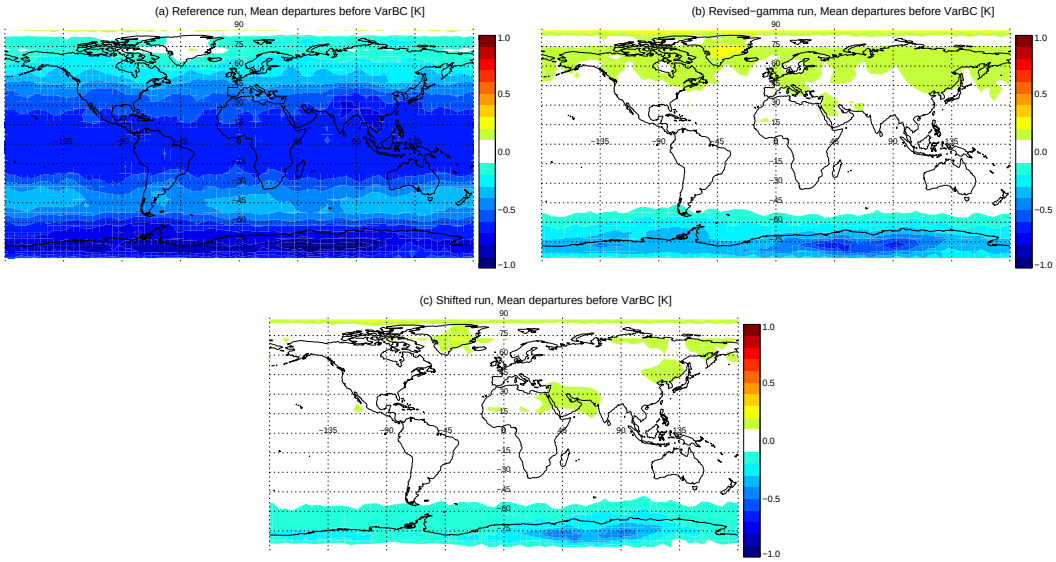

Figure 7: Mean of first-guess departures before bias correction for assimilated AMSU-A on NOAA-18 channel 7 in the: a) 'Reference run'; b) 'Revised-γ run'; c) 'Shifted run'. The sample is based on the period 1 to 31 August 2013.

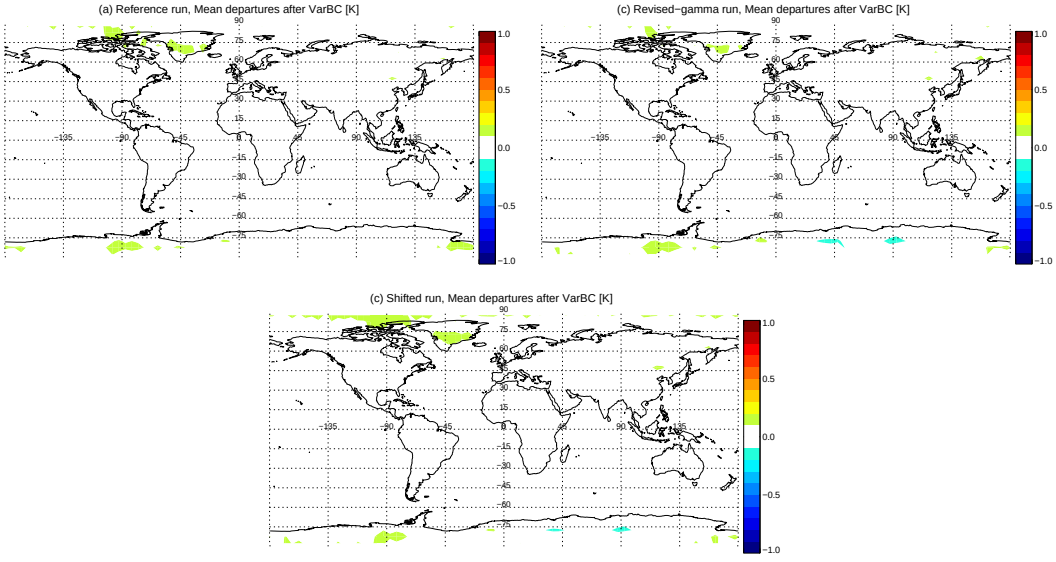

Figure 8: Same as Figure 7 but after bias correction.

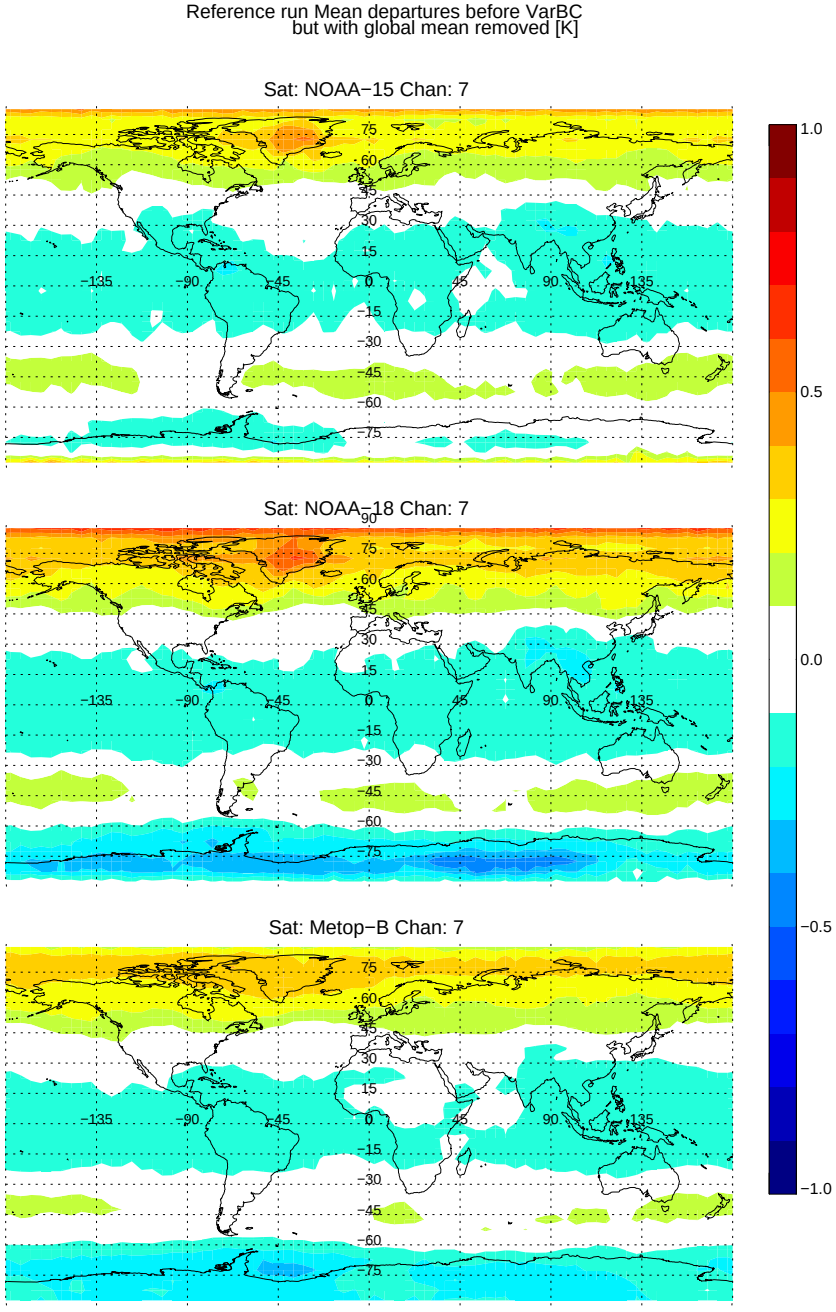

Figure 9: Mean of first-guess departures before bias correction in AMSU-A channel 7, binned to a 5°latitude-longitude grid, but with the mean bias correction removed. The sample is based on the period 1 to 31 August 2013. These departures are taken from the 'Reference run' for AMSU-A on three satellites (e.g., NOAA-15, NOAA-18 and MetOp-B).

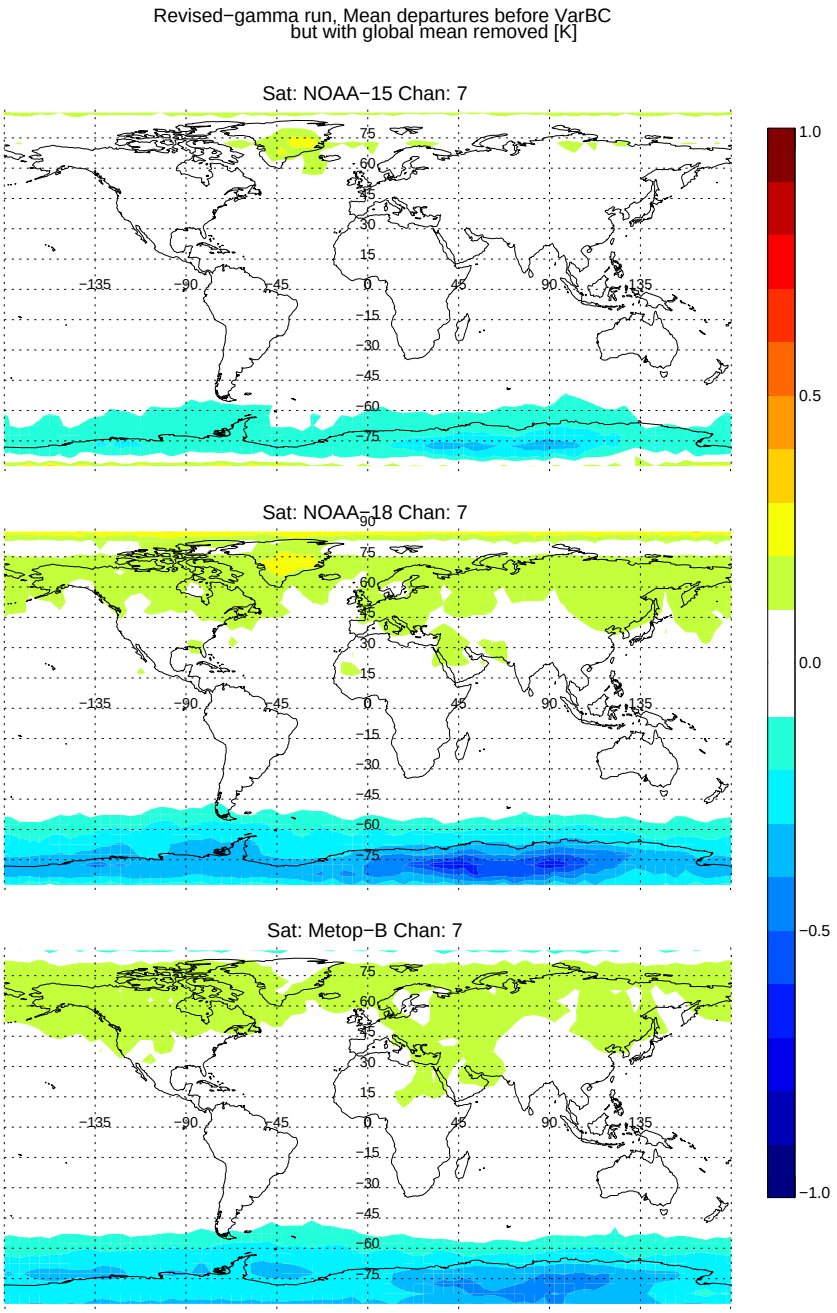

Figure 10: Same as Figure 9 but, the departures are taken from the 'Revised-γ run'.

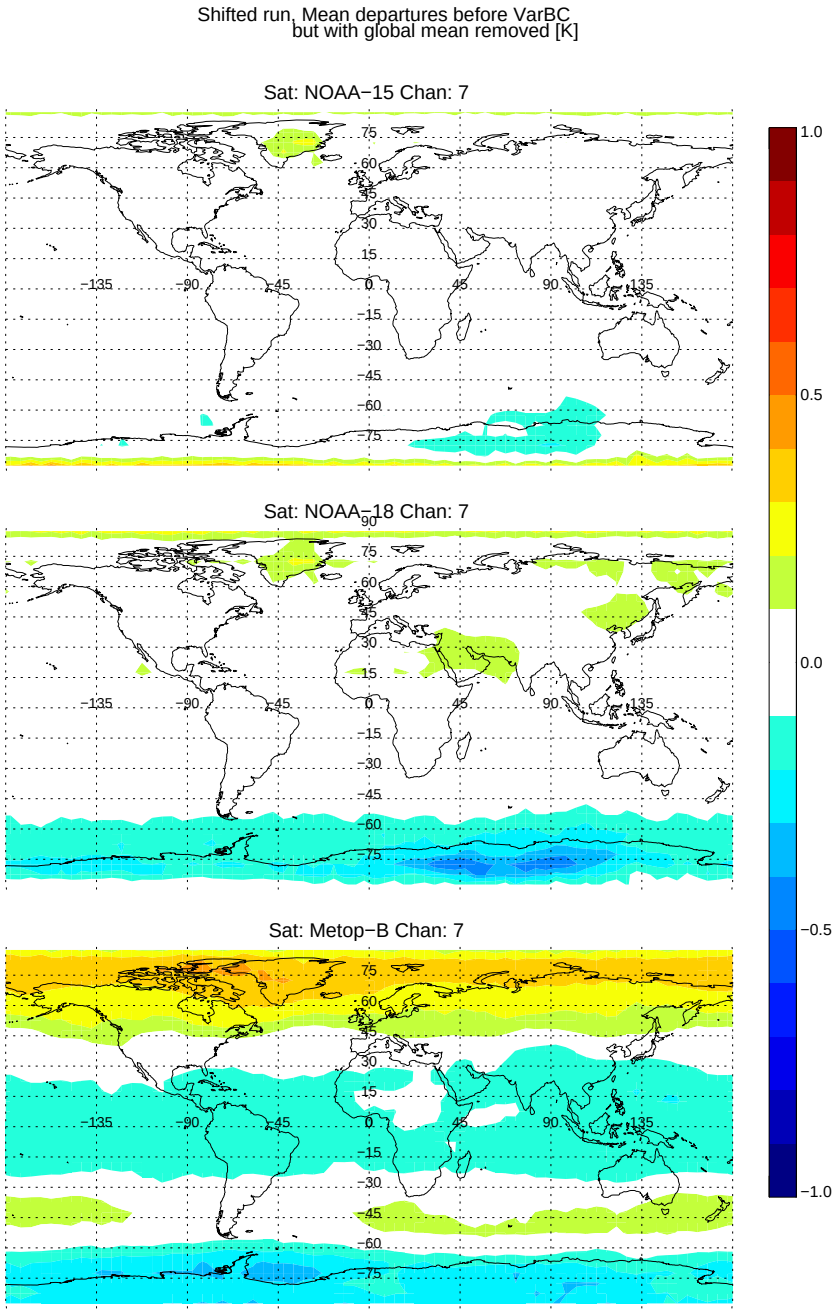

Figure 11: Same as Figure 9 but, the departures are taken from the 'Shifted run'. Note that no passband shift is applied to Metop-B.

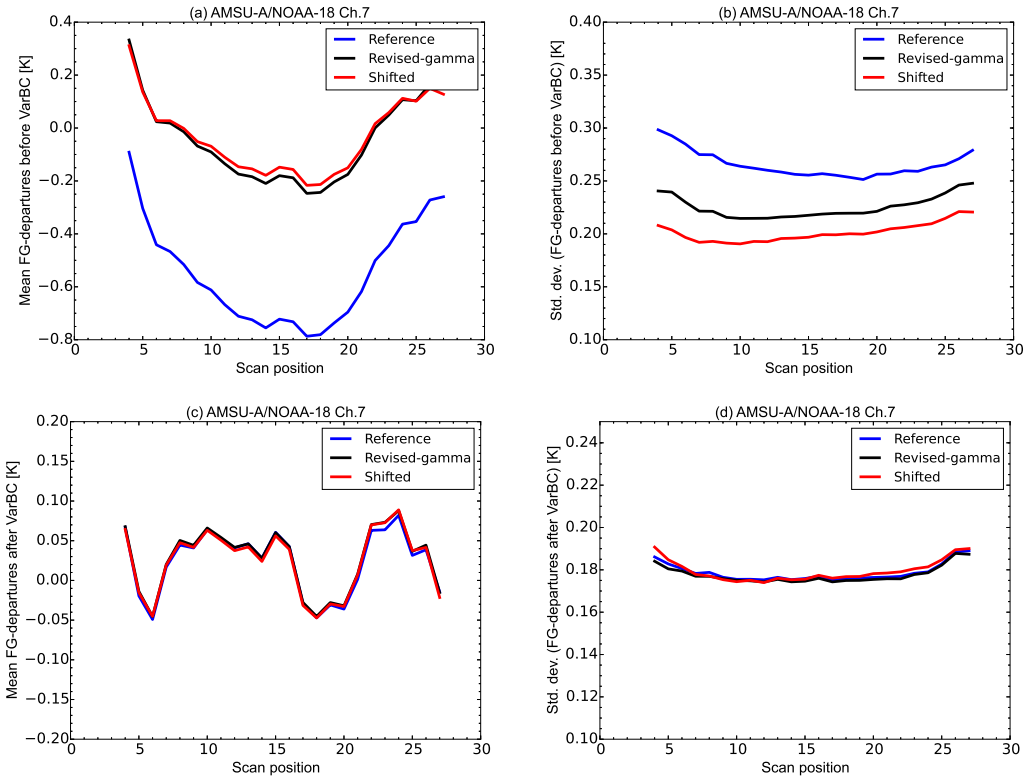

Figure 12: Mean (left) and standard deviations (right) of FG-departures, before (top) and after (bottom) the bias correction, as a function of scan position for AMSU-A on NOAA-18 channel 7 during August 2013. The outermost 3 AMSU-A scan-positions on either side are currently not assimilated at ECMWF and statistics are based on antenna-corrected data. The scaling factor for the optical depths in the radiative transfer calculations is γ=1 in the 'Reference run' (blue line), γ = 1.34 in the 'Revised-γ run' (black line) while a 30 MHz shift in the passband center frequencies is applied in the 'Shifted run' (red line).

aggregated together during the period 1 August 2013 - 28 February 2014. Using the revised γ-values with the AMSU-A coefficient files generally reduces the standard deviation of the FG departures relative to the 'Reference run' in channels 5 to 8 for individual AMSU-A sensors. The most significant improvement is found in AMSU-A channel 8 (i.e., MetOp-A, -B, NOAA-15, -18, Aqua) where a reduction in the standard deviation of first guess departures up to 3% is seen. For channel 9 and above, any change in the standard deviation of the FG departures is relatively small and is not statistically significant.

Accounting for a passband shift in AMSU-A coefficient files gives more mixed results. For example, a shift of 52 MHz from the nominal passband center frequency of 54.94 GHz for NOAA-16 channel 7 results in a significant reduction in the standard deviation of the FG departures of 8%. Furthermore, a shift of 27 MHz from the nominal passband center frequency of 55.50 GHz for NOAA-15 channel 8 results in a reduction in the standard deviation of the FG departures of 3%. Smaller improvements in the FG standard deviation of up to 1% are seen for AMSU-A channel 8 on MetOp-A and Aqua and AMSU-A channel 6 on NOAA-19. There is an increase in the FG standard deviation for AMSU-A channel 7 on NOAA-18 (1%) where a shift of 30 MHz from the nominal passband center frequency has been assumed and for AMSU-A channel 8 on MetOp-B (3%) where no shifted passband have been assumed relative to nominal values. The one situation where passband shifts are clearly better than γ-corrections is for

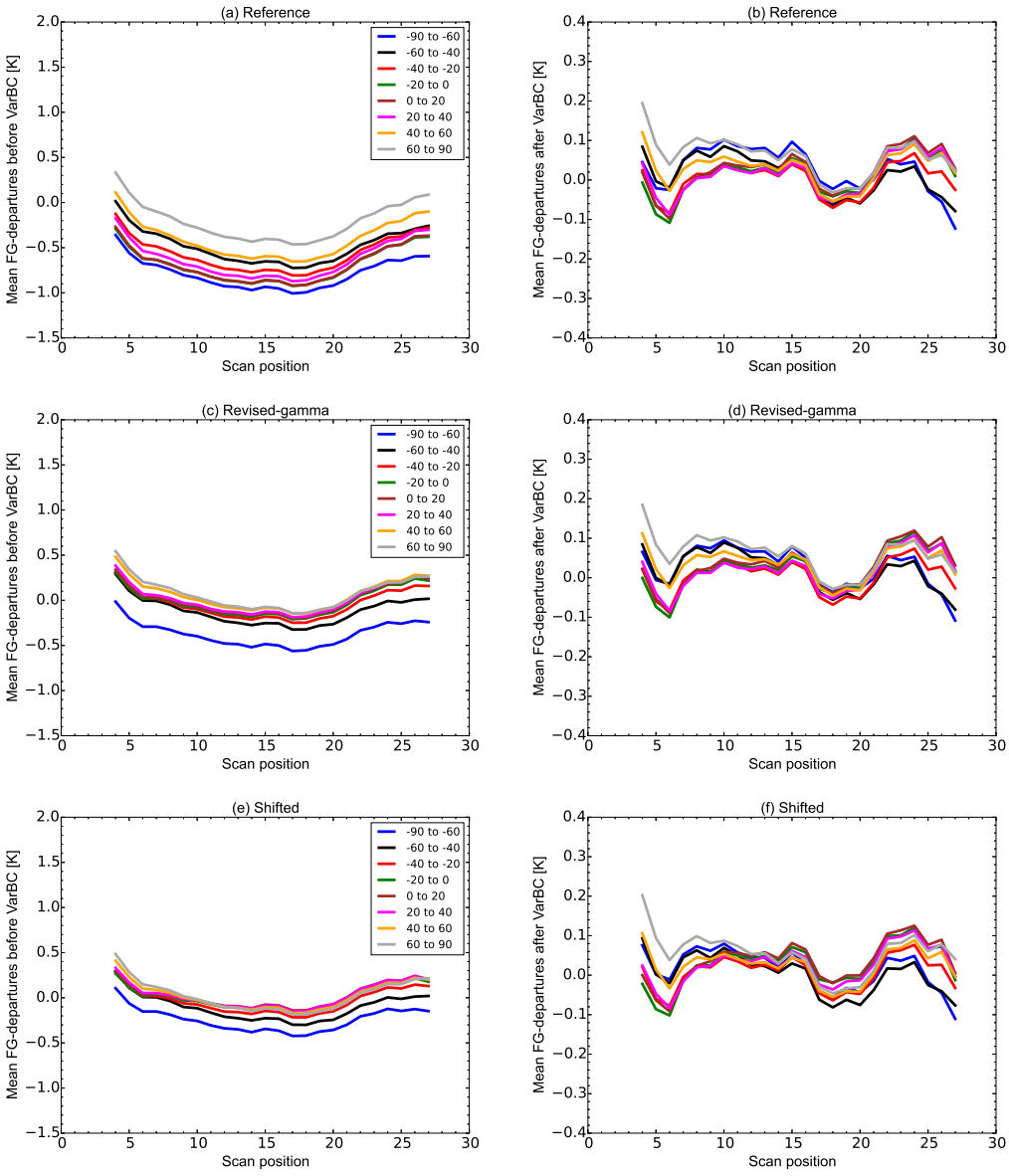

Figure 13: Mean of FG-departures before (left) and after (right) the bias correction, as a function of scan position for AMSU-A on NOAA-18 channel 7 during August 2013. Statistics are based on antenna-corrected data in all three runs: 'Reference' (top), 'Revised-γ' (middle) and 'Shifted' (bottom).

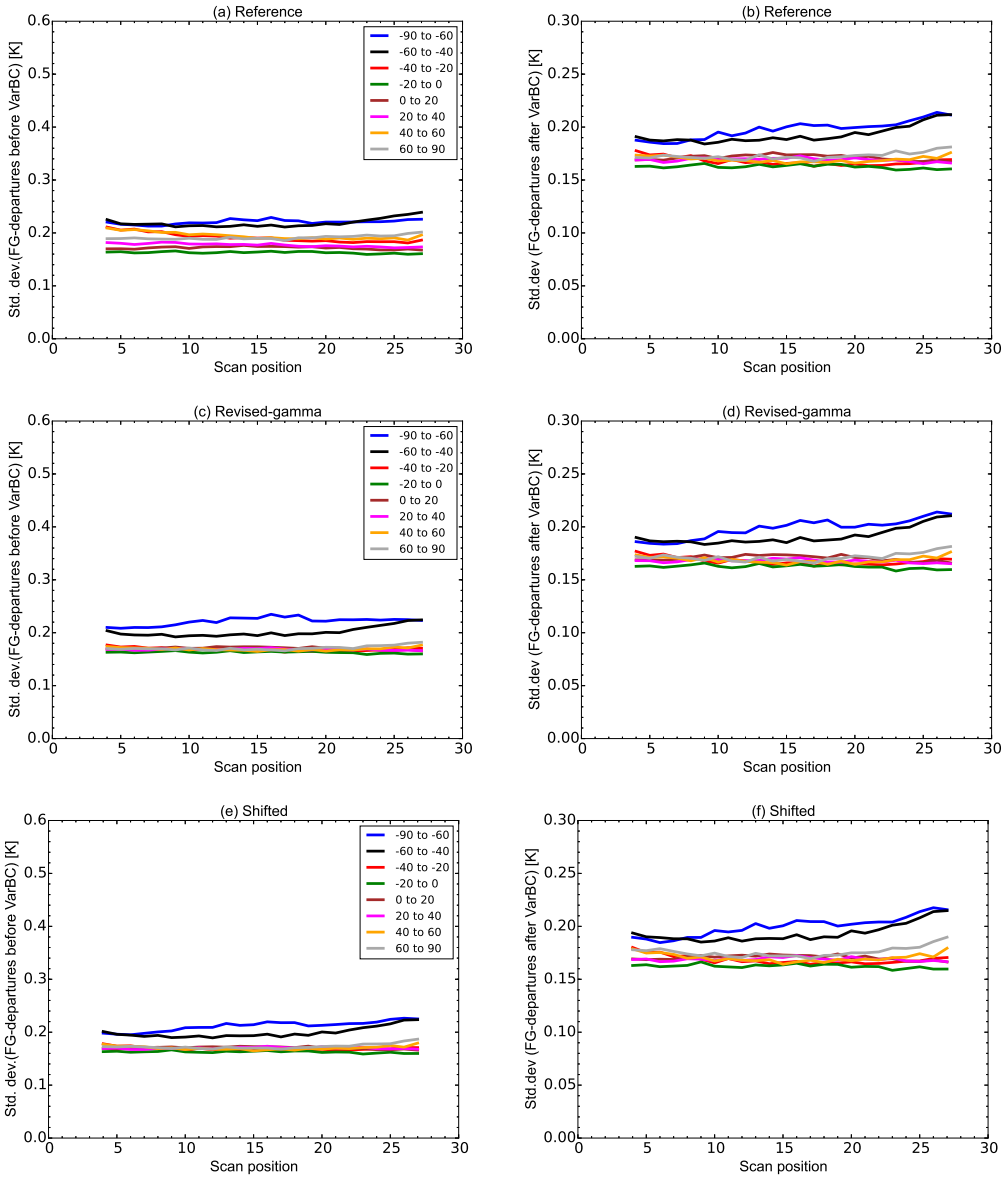

Figure 14: Standard deviations of FG-departures before (left) and after (right) the bias correction, as a function of scan position for AMSU-A on NOAA-18 channel 7 during August 2013. Statistics are based on antenna-corrected data in all three runs: 'Reference' (top), 'Revised-γ' (middle) and 'Shifted' (bottom).

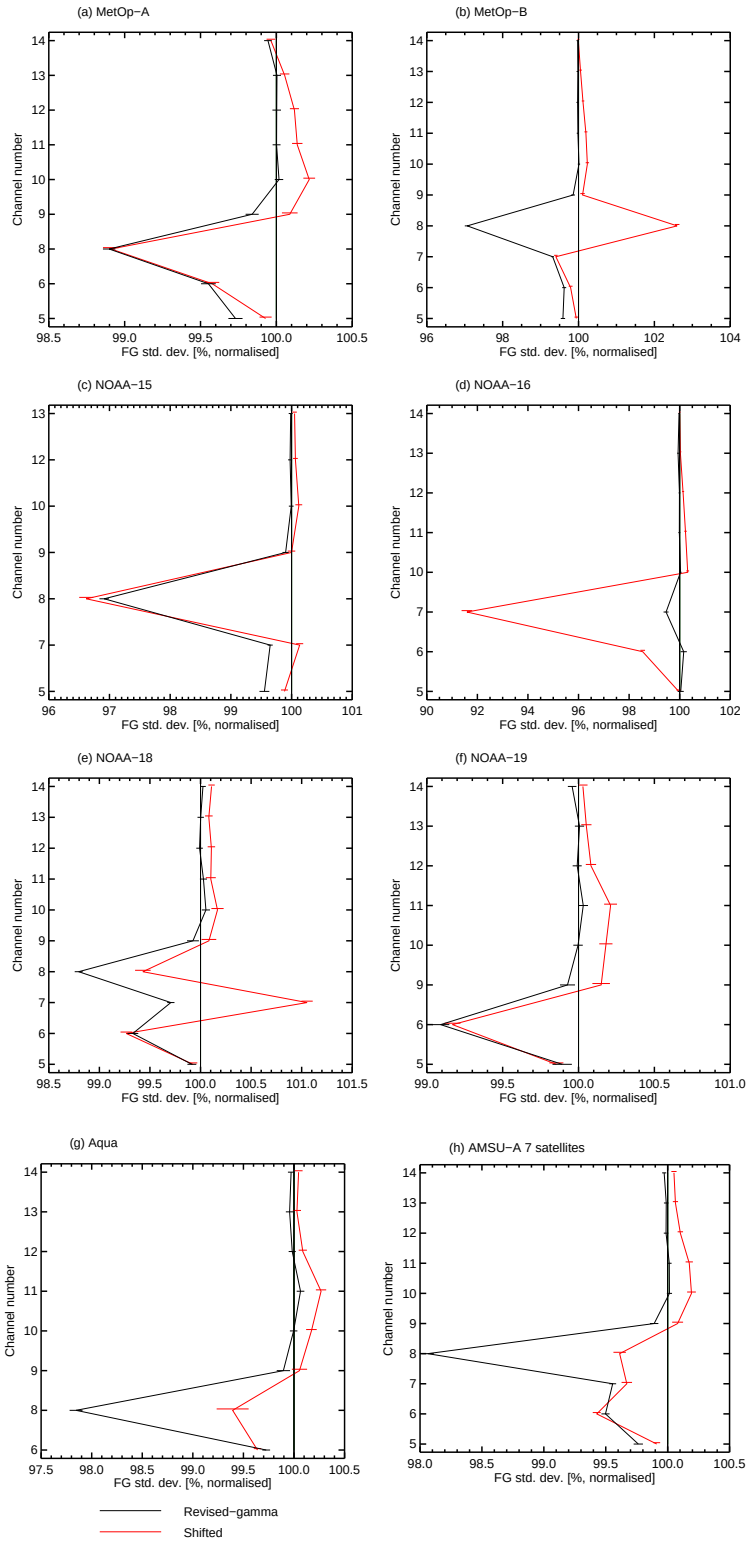

Figure 15: Normalised standard deviations of first guess departures for each of the actively assimilated AMSU-A sensors and combined over all AMSU-A's during the period 1 August 2013 - 28 February 2014: a) MetOp-A; b) MetOp-B; c) NOAA-15; d) NOAA-16; e) NOAA-18 f) NOAA-19; g) Aqua and h) combined across all seven AMSU-A instruments. Statistics are calculated over the globe and the normalisation is with respect to the standard deviations of the 'Reference run'. Values below 100% indicate smaller standard deviations when γ- or passband shifts information has been incorporated into the ECMWF radiative transfer modelling. The error bars indicate a 95% statistical confidence interval.

NOAA-16, where the γ-corrections are ineffective at reducing standard deviations.

Global results for all AMSU-A sensors aggregated together are shown in Figure 15h. The FG standard deviations are reduced in the 'Shifted run' by up to 0.5% in channels 6-8, but degraded by up to 0.2% for channels 9-12, an issue that is also seen for all the individual sensors. The largest reduction in the FG standard deviation is for channel 8 in the Tropics and channel 6 in the midlatitudes (by up to 0.9% and by 0.6%, respectively, not shown). The 'Revised-γ run' is significantly better in improving the fit of FG forecasts to AMSU-A observations and has a pronounced impact around and above the tropopause. The greatest impact is in AMSU-A channel 8 (by up to 2%).

Because the presence of bias correction can obscure the full effect of the γ and passband shifts on biases, Figure 16 shows the standard deviation of first-guess departures before variational bias correction, comparing the effect of γ-corrections or shifted passbands relative to those from the control for August 2013. Although the magnitude of the reductions in standard deviation are much larger, in general conclusions are similar to those from the bias-corrected results. Although reductions in the standard deviations of first-guess departures are achieved in some cases for AMSU-A channels peaking in the lower troposphere, the standard deviation of the FG-departures increases for AMSU-A channels 9 to 12 on all platforms, even for the γ corrections. These also give an increase in the standard deviation of first-guess departures for AMSU-A channel 6 on NOAA-18, -19, MetOp-A and MetOp-B. This is also noticed for both AMSU-A channels 5 and 6 in the 'Shifted' run.

Figure 17 shows global mean biases before VarBC correction. Because these are cycling data assimilation experiments, channels 9 – 14 do not give identical results between the three available sets coefficient files, and instead there are some small mean shifts. It is interesting that most sensors show similar patterns of bias across these channels with NOAA-18 being an outlier. Channels 5 – 8 show different biases on different instruments, reflecting some of the inter-satellite biases investigated by Zou and Wang (2011). As already seen, one effect of γ-correction and passband shifts is around a 0.5 K decrease in simulated brightness temperatures (which translates to an increase in FG departure). This shift reduces mean biases for some channels and increases it for others, depending on the relative bias of each satellite. This is one reason why this study focuses on the air-mass dependent part of the bias and allows VarBC to correct the global biases.

The effect of the γ-correction and passband shifts on the standard deviation of fits in channels 9 and 10 is of concern. No additional correction has been applied to these channels, so this increase in standard deviation suggests an increased discrepancy between the short-range forecast and the AMSU-A observations due to changes in the short-range forecast. Figure 5 shows that channel 9 is affected by air-mass dependent biases that are of similar nature, but smaller than those in channel 8. Previous work has found that these air-mass biases shown in channel 9 cannot be addressed through a γ-correction or a passband shift (Watts and McNally, 2004; Lu and Bell, 2014). This suggests another source of the bias for channel 9 (e.g., forecast model bias or a different type of radiative transfer bias). It may be that this bias also affects the lower channels, and that it has been aliased incorrectly into the estimates for the gamma correction or the pass-band shift, leading to the observed inconsistency.

To further support the results presented so far, we have also conducted additional monitoring experiments in which the same FG is used to calculate model equivalents for the three different sets of AMSU-A coefficient files (i.e., previously described in section 4.1). This allows us to examine the characterisation of biases without the interaction between model fields and bias corrections otherwise present in the assimilation experiments. This analysis confirms the results already presented. For example, the pattern of the mean value of the difference between observed and computed AMSU-A brightness temperatures is consistent between the mid-upper tropospheric sounding channels (6 – 8) and the stratospheric channels

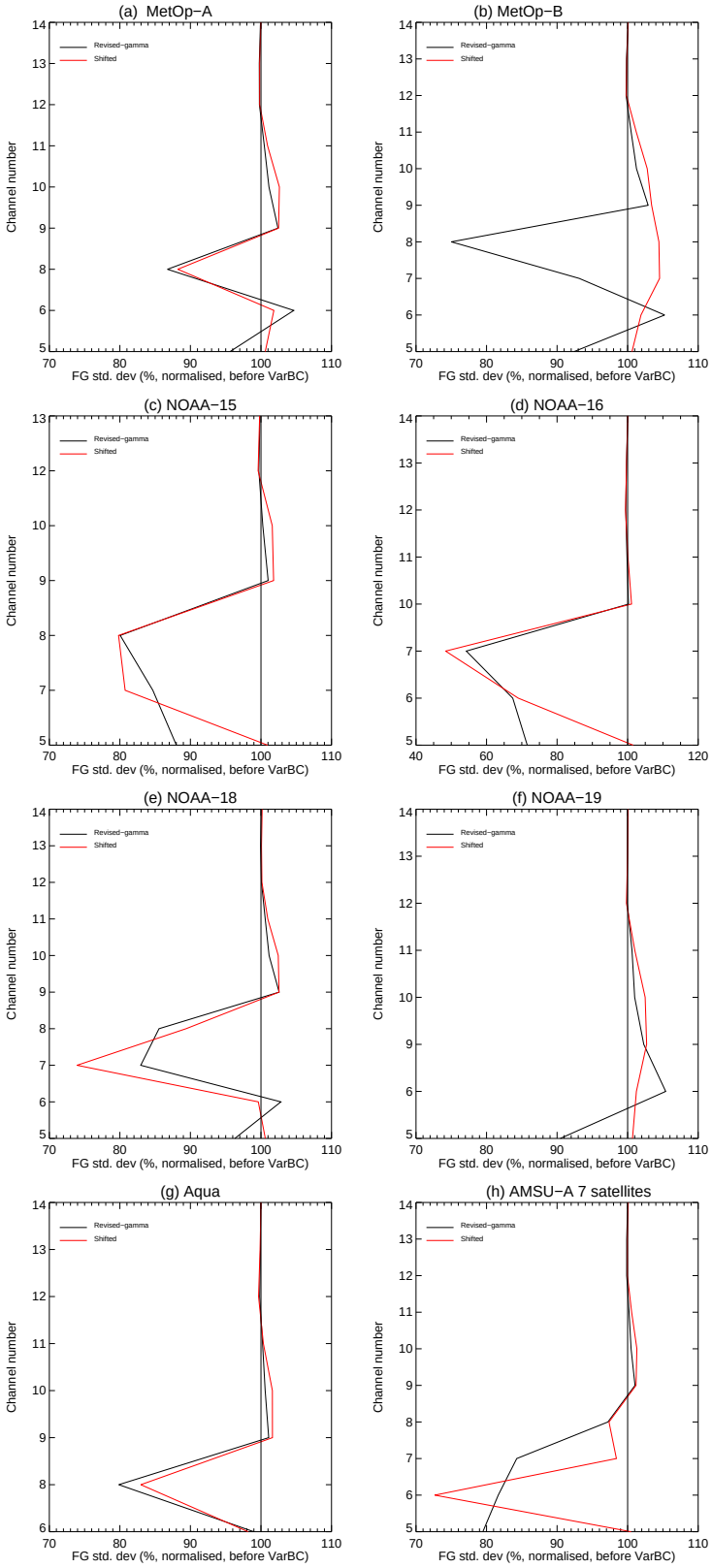

Figure 16: Same as Figure 15 but before the variational bias correction during August 2013. Note that, except for NOAA-16 in panel c), the x-axis ranges from 70% to 110%.

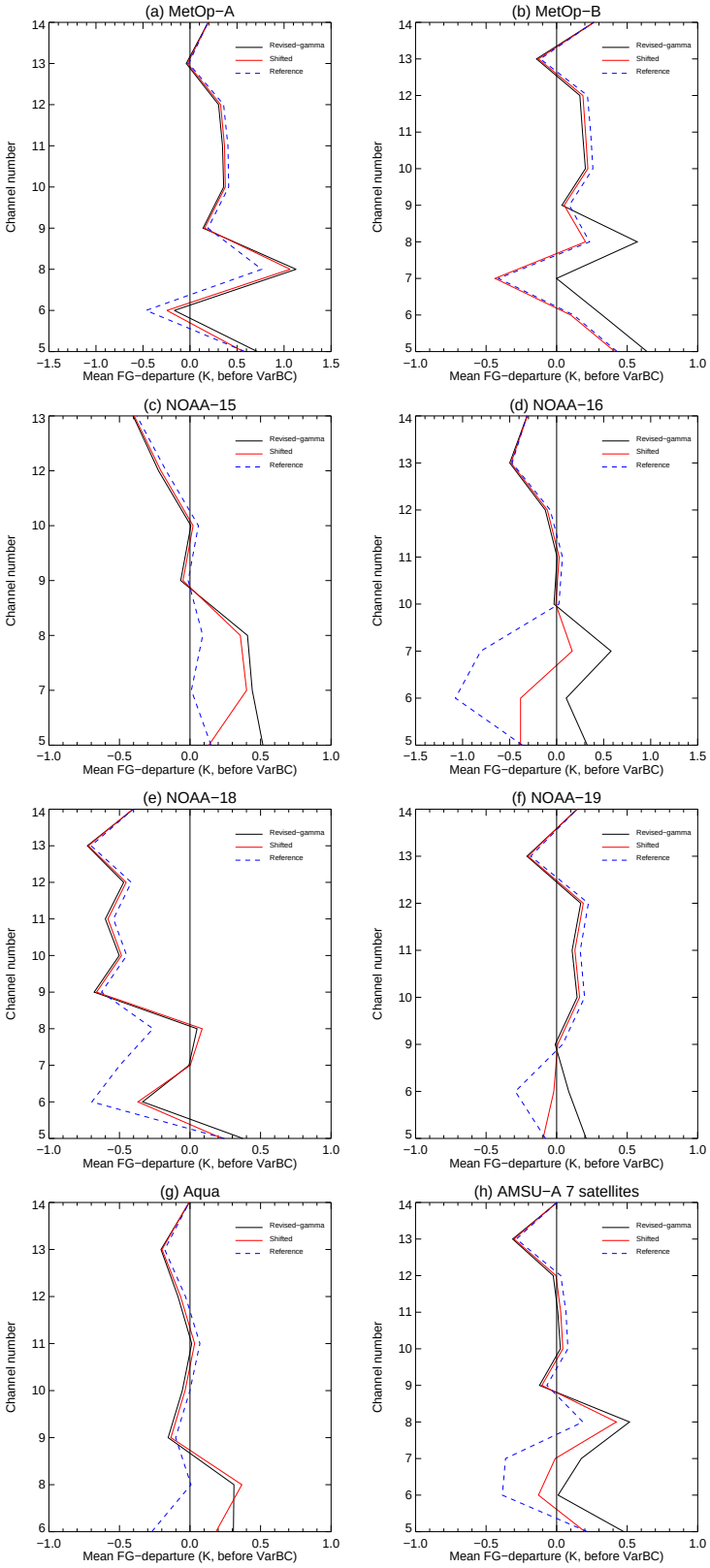

Figure 17: Mean FG-departures before bias correction for each of the actively assimilated AMSU-A sensors and combined over all AMSU-A's for August 2013: a) MetOp-A; b) MetOp-B; c) NOAA-15; d) NOAA-16; e) NOAA-18 f) NOAA-19; g) Aqua and h) combined across all seven AMSU-A instruments. Statistics are calculated over the globe.

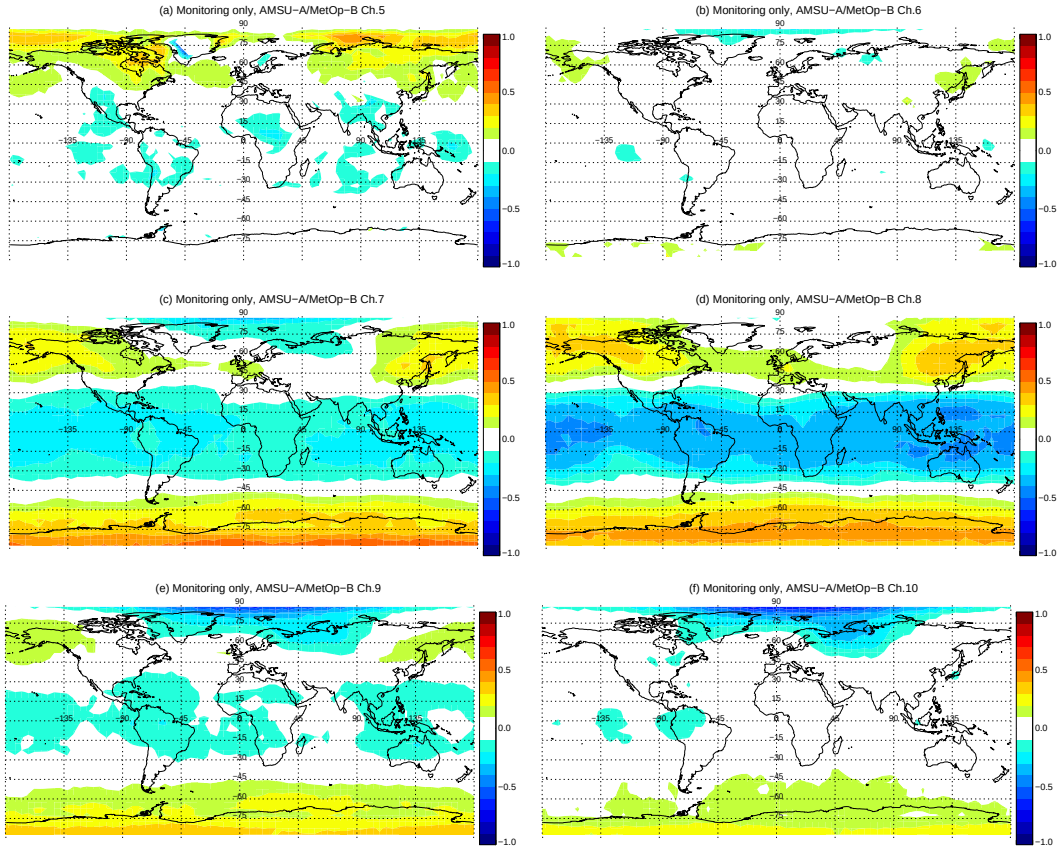

Figure 18: Mean of first-guess departures before bias correction, binned to a 5°latitude-longitude grid, but with the mean bias correction removed for AMSU-A on MetOp-B channels 5 to 10 from the 'Reference run' monitoring only experiment. The sample is based on the period 1 to 28 February 2014.

(9 – 14). An example is shown in Figure 18 for AMSU-A channels 8 and 9 on MetOp-A. Also, we have chosen here to present results from February 2013 to illustrate how the negative bias associated with the polar vortex is now seen in the northern hemisphere, and the positive bias associated with the relatively isothermal lower stratosphere of polar summer is now observed in the south. In the rest of this study we rely on the active assimilation experiments because the impact of the γ-correction and/or passband shifts on active data assimilation is our primary interest here.

4.3 Fits to other observations and changes in temperature analysis

First-guess fits to ATMS on S-NPP observations are shown in Figure 19a). ATMS channels 6 to 15 are similar to AMSU-A channels 5 to 14, but the RTTOV coefficient files are the same for this instrument for the three assimilation experiments. Unlike AMSU-A, which has a separate stabilised local oscillator for channels 3 – 8 and 15 and a phase-locked oscillator for channels 9 – 14, ATMS channels share all the same phase-locked oscillator. Both 'Revised-γ run' and 'Shifted run' show improved FG fits for ATMS channels 6 to 9 globally. We found approximately 2.7% and 1.8% significant improvements of the FG fit in ATMS channel 9 in the 'Shifted run' and 'Revised-γ run', respectively. Consistent with the

AMSU-A results, the standard deviation of the FG departures channels 10 to 15 increase of up to 0.2% in the 'Shifted run', while there was no impact on background fits in the 'Revised-γ run'.

Fits to IASI from Metop-A, AMVs combining statistics from both u- and v-wind components and radiosondes temperature observations are also analysed through Figures 19b)- 19d). The 'Shifted run' brings statistically significant improvements in standard deviations of FG departures for AMVs below 500 hPa and for radiosonde temperature observations between 200 hPa and 500 hPa. However, some degradations of around 0.1-0.2% in standard deviations of FG departures are noticed for IASI stratospheric channels, consistent with degradations in the ATMS stratospheric channels. A broadly similar picture is seen in AMVs between 300 and 500 hPa and for the radiosondes temperature observations at 150 hPa where FG fits show degradations of around 0.2%. The 'Revised-γ run' also shows generally beneficial impacts but has increased standard deviation of FG departures in a few situations: for AMVs at 400 hPa and radiosondes temperature observations at 700 hPa.

The zonal mean cross section of the difference between the temperature analysis of the γ- or passband shifts runs and the reference run are shown in Figure 20. There is a slight warming around and above the tropopause and a cooling in the layers below over the high latitudes with changes to the mean analysis of temperature less than 0.1 K for both experiments. This appears relatively insignificant given that the γ-corrections or passband shifts are correcting biases of up to order 1 K (see e.g. Figure 7).

4.4 Forecast impact

The impact on forecasts of using revised AMSU-A coefficient files is assessed in this section. As an example, Figure 21 shows results in terms of 500 hPa geopotential height and 100 hPa temperature and wind vector for the extratropical northern and southern hemispheres and for the tropics. In the midlatitudes, both the 'Shifted run' and 'Revised-γ run' have a beneficial impact on 500 hPa geopotential height in the short-range (T+12-h to T+36-h) and a not beneficial impact after the day two forecasts. Similarly, the impact on temperature and wind at 100 hPa is beneficial in the 'Revised-γ run' in the short-range and not beneficial at longer range. The 'Shifted run' gives a stronger increase in temperature and wind standard deviation forecast error at 100 hPa than the 'Revised-γ run', especially in the short-range. Given the small size of the forecast impact relative to the confidence range, these results do not show any statistical significance between the two experiments: we cannot conclude as to whether Revised-γ or Shifted coefficients are best from these results.

The normalised changes in standard deviation errors in temperature and wind as a function of latitude and pressure are shown in Figures 22– 23 and Figures 24– 25, respectively. Using AMSU-A regression coefficient files accounting for the revised γ-values results in a statistical significant improvement in forecast errors up to day 2 when each experiment is verified against its own analysis (Figure 22). However, temperature errors in the southern hemisphere between 10 and 100 hPa show a significant degradation at day 3. Some degradations, not statistically significant, persist in midlatitudes in the upper and lower troposphere to the end of the forecast range. The wind forecast impact is beneficial in the short-range but not at the longer range. Figure 24 shows statistically significant degradations below 100 hPa over mid-latitudes extratropics from day 2 onwards.

Using shifted channel centre frequencies for AMSU-A tropospheric channels 6 – 8 has a significant beneficial impact up to day 1 in forecast scores of temperature in the lower troposphere. Nonetheless, there are a small number of significantly negative values above 150 hPa (Figure 23). The signal was also present in the observation fits. A very significant degradation in forecast scores of both, temperature

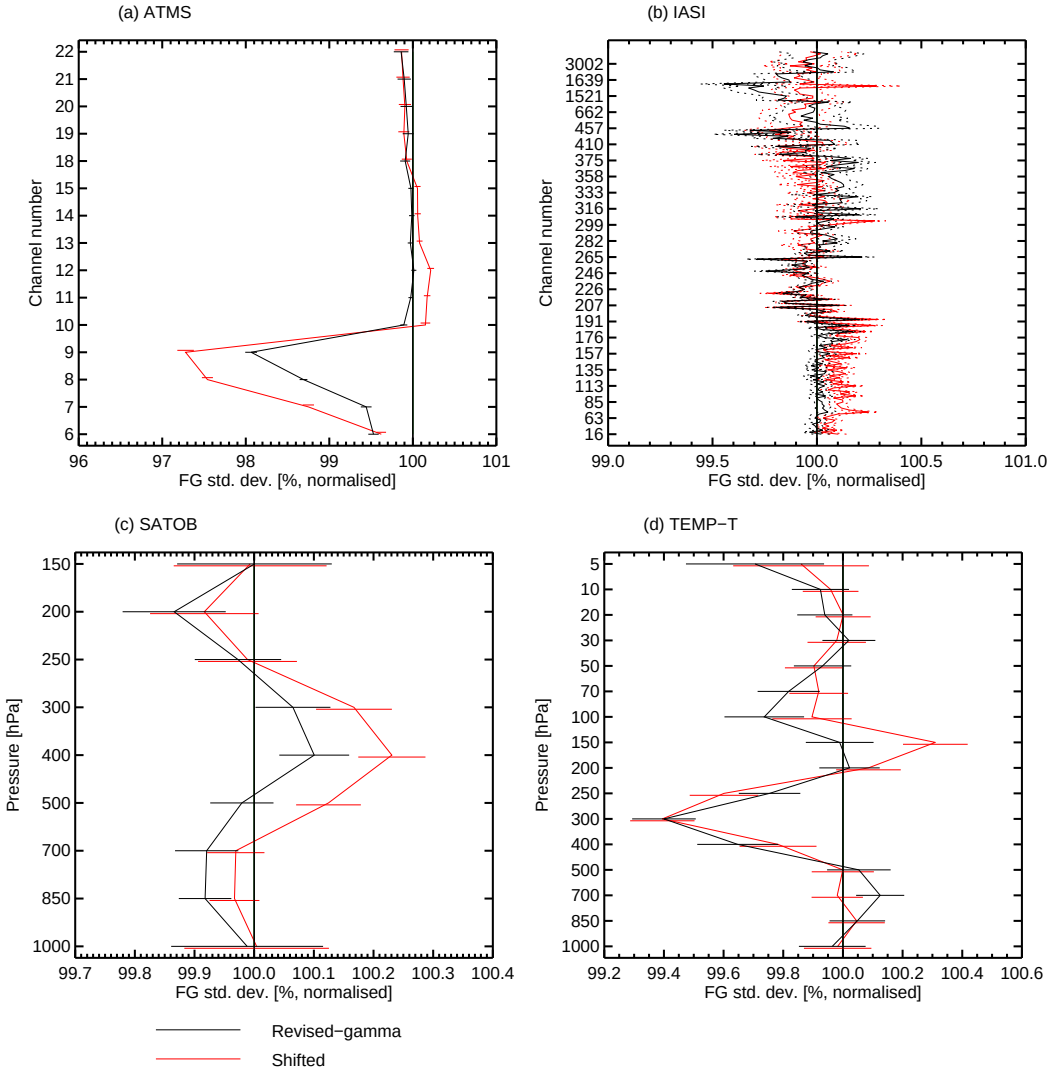

Figure 19: Normalised standard deviation of first-guess departures as a percentage relative to the control for: a) ATMS on S-NPP observations; c) IASI on MetOp-A/B observations; c) Atmospheric Motion Vectors combining statistics from u- and v- components and d) Temp-T radiosonde observations. The area is global and the period is from 1 August 2013 to 28 February 2014. Error bars indicate the 95% confidence interval. Numbers less than 100% indicate beneficial impact, i.e. smaller standard deviations when γ- or passband shift information has been incorporated into the ECMWF radiative transfer modelling.

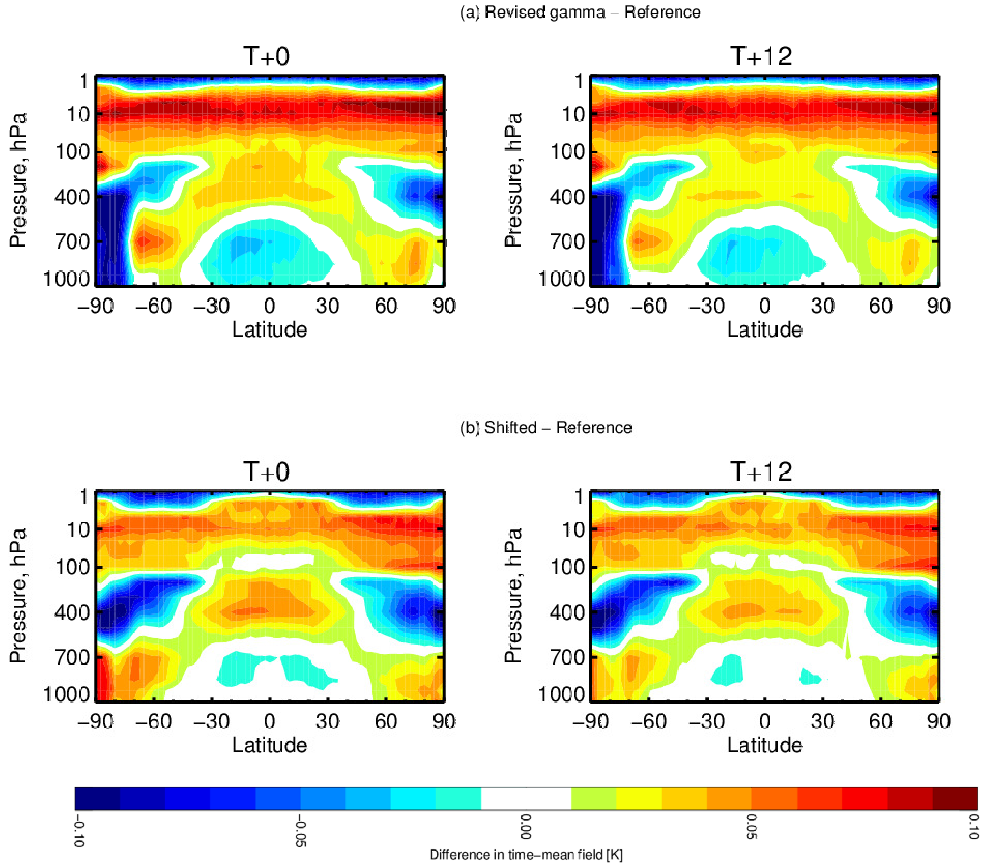

Figure 20: Difference in the zonal mean temperature analysis and forecasts [K] between: (a) the Revised-gamma run and the Reference run; (b) the Shifted run and the Reference run. The positive values, displayed in red colors, indicate warmer values in the Revised-gamma and the Shifted run, respectively.

(Figure 23) and wind (Figure 25) is noticed from day 2 to day 5, in particular in the southern hemisphere.

In summary, considerable changes in the medium range forecast scores were found for both 'Revised-γ run' and 'Shifted run'. The reduction in short-range forecast errors, when measured against own-analyses, is consistent with the reduction in the size of the first-guess departures that can be achieved by either of these corrections. However, in the medium-range forecast, persistent degradations of the forecast scores of temperature, wind and geopotential height field are seen in the midlatitudes and in the upper troposphere.

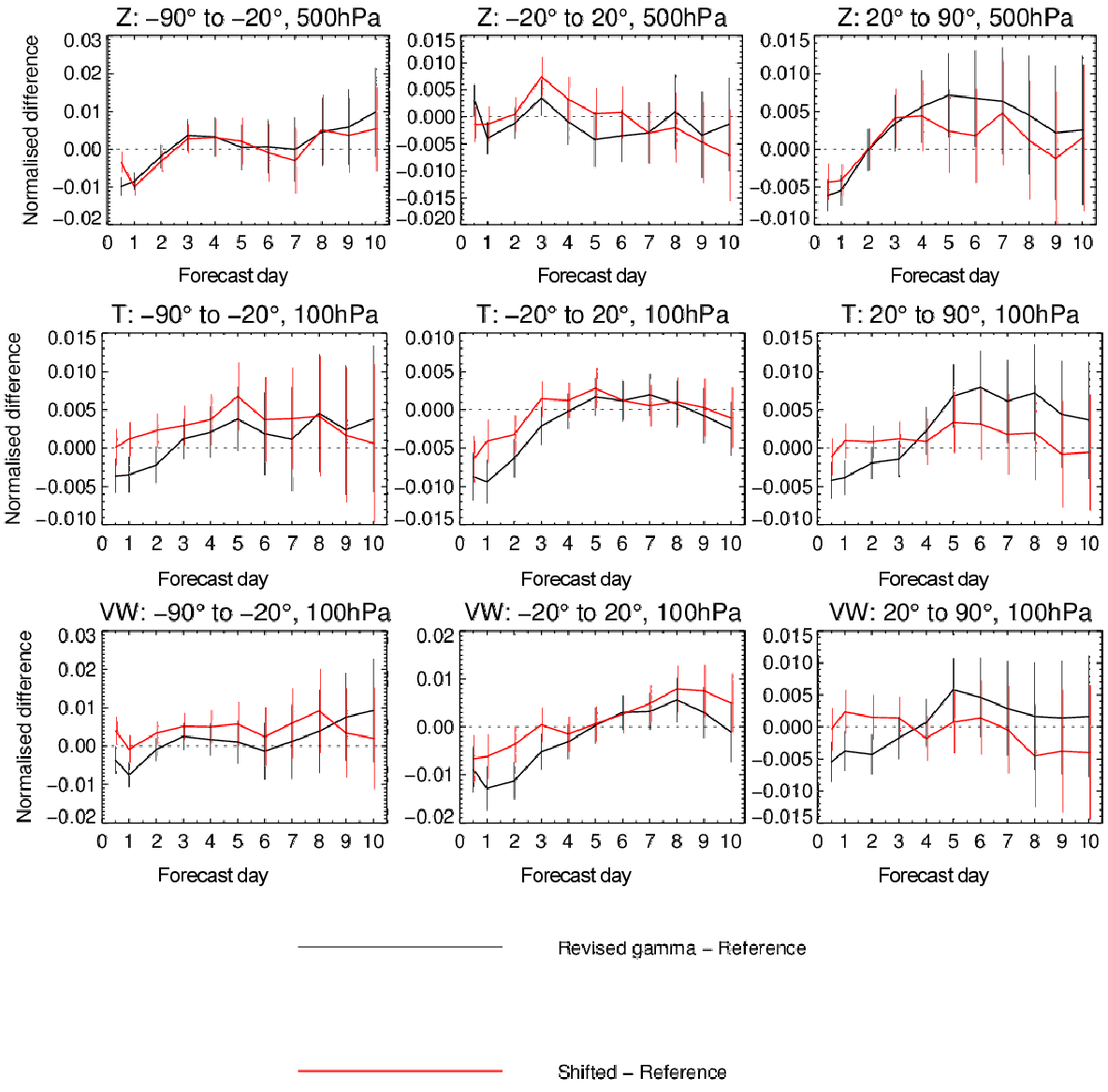

Figure 21: Normalized differences in the standard deviation forecast error as a function of forecast range (days) for the three experiments. The black line indicate differences between the 'Revised-γ run' and the 'Reference run', while the red line between the 'Shifted run' and the 'Reference run', as indicated in the legend. Results are based on 404 to 423 forecasts depending on the forecast range over seven month period, August 2013 to February 2014. The vertical bars indicate 95% confidence intervals for the indicated score differences. Verification is against own analysis. First row: for the 500hPa geopotential over the Southern Hemisphere extratropics (left side), Tropics (middle) and the Northern Hemisphere extratropics (right side); Second row: for the 100hPa temperature forecast; Third row: for the 100hPa wind forecast; Negative values indicate a reduction in forecast error and hence a beneficial impact on forecasts.

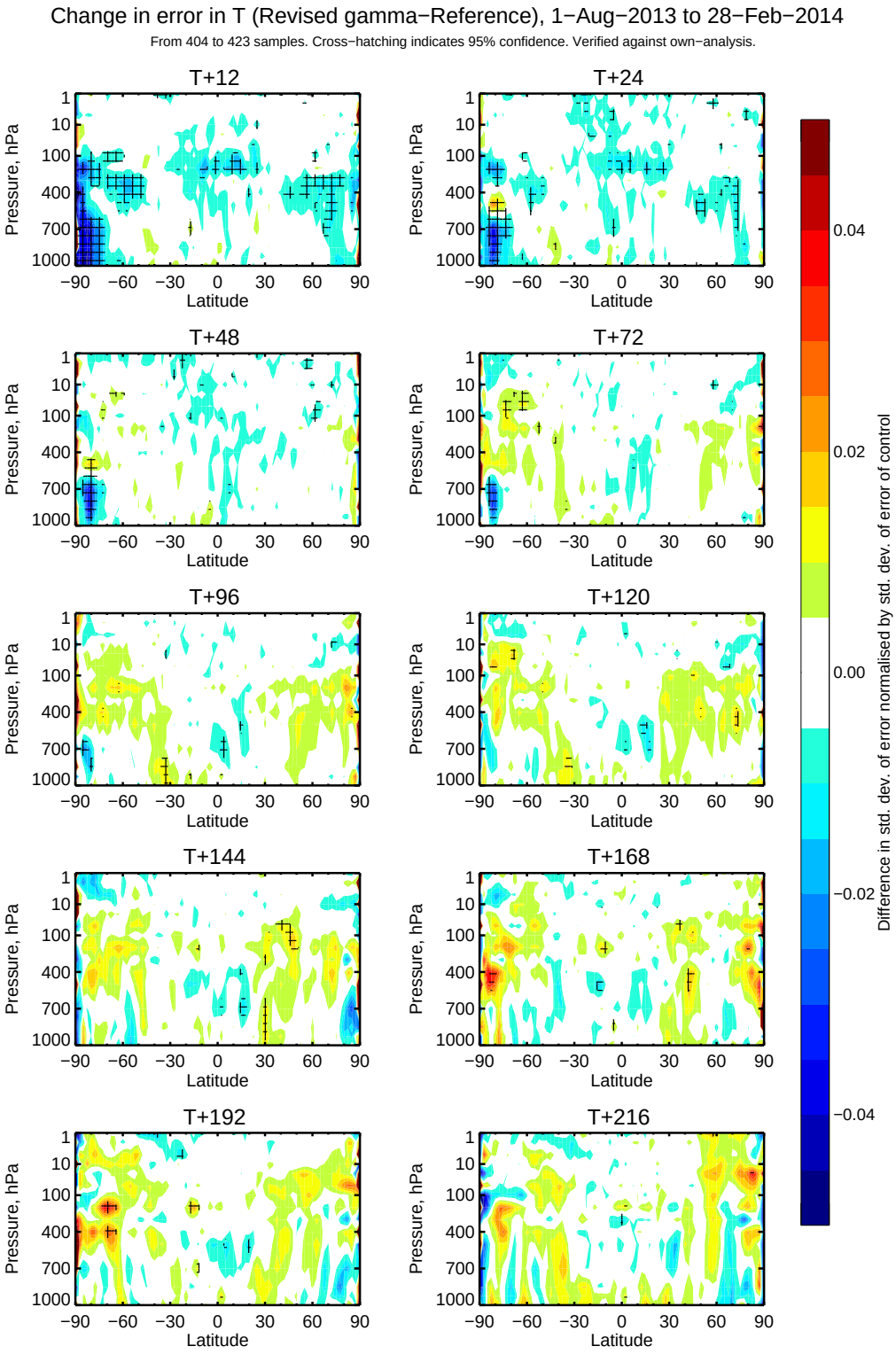

Figure 22: Normalised change in the standard deviation of temperature forecast error between the 'Revised-γ run' and the 'Reference run'. Verification is against own analysis and scores are based on the combined 7 months of experimentation, August 2013 to February 2014. Cross-hatched areas show changes that are significant at the 95% confidence level. Negative values (blue areas) indicate reduced standard deviation in the 'Revised-γ run' and hence improved forecasts compared to the Reference run'.

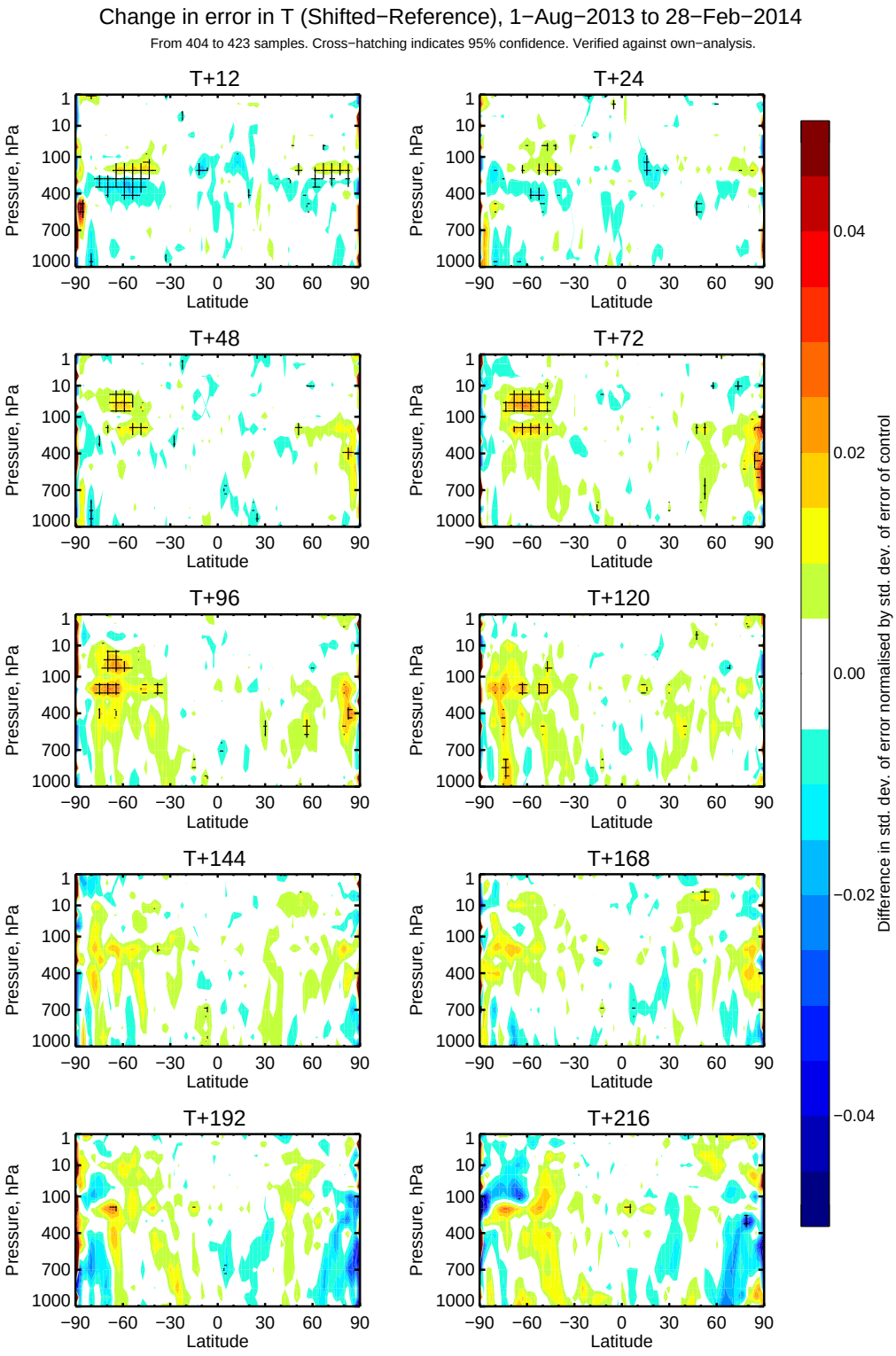

Figure 23: Same as Figure 22 but, between the 'Shifted run' and the 'Reference run'.

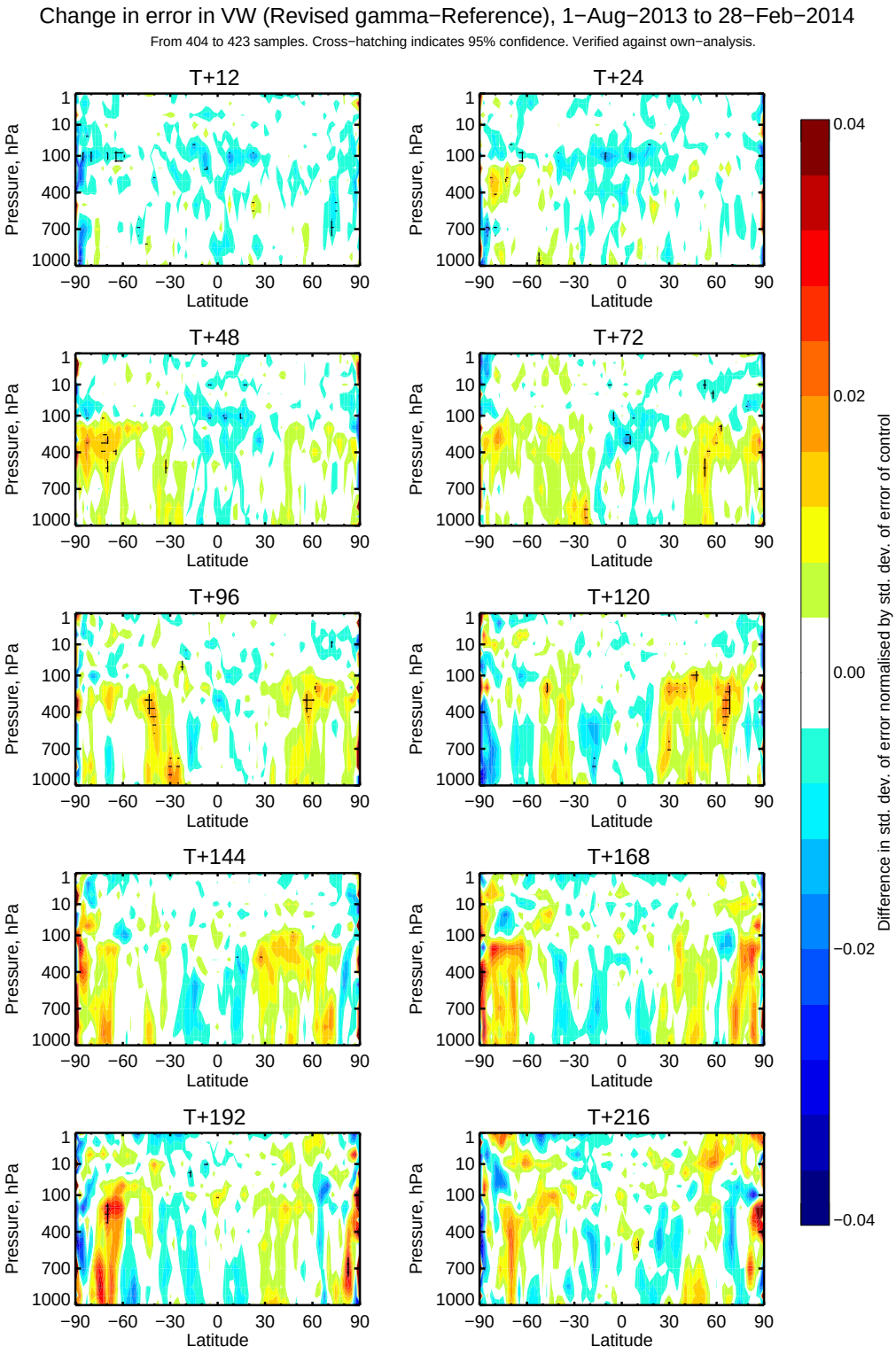

Figure 24: Normalised change in the standard deviation of vector wind forecast error between the 'Revised-γ run' and the 'Reference run'. Verification is against own analysis and scores are based on the combined 7 months of experimentation, August 2013 to February 2014. Cross-hatched areas show changes that are significant at the 95% confidence level. Negative values (blue areas) indicate reduced standard deviation in the 'Revised-γ run' and hence improved forecasts compared to the 'Reference run'.

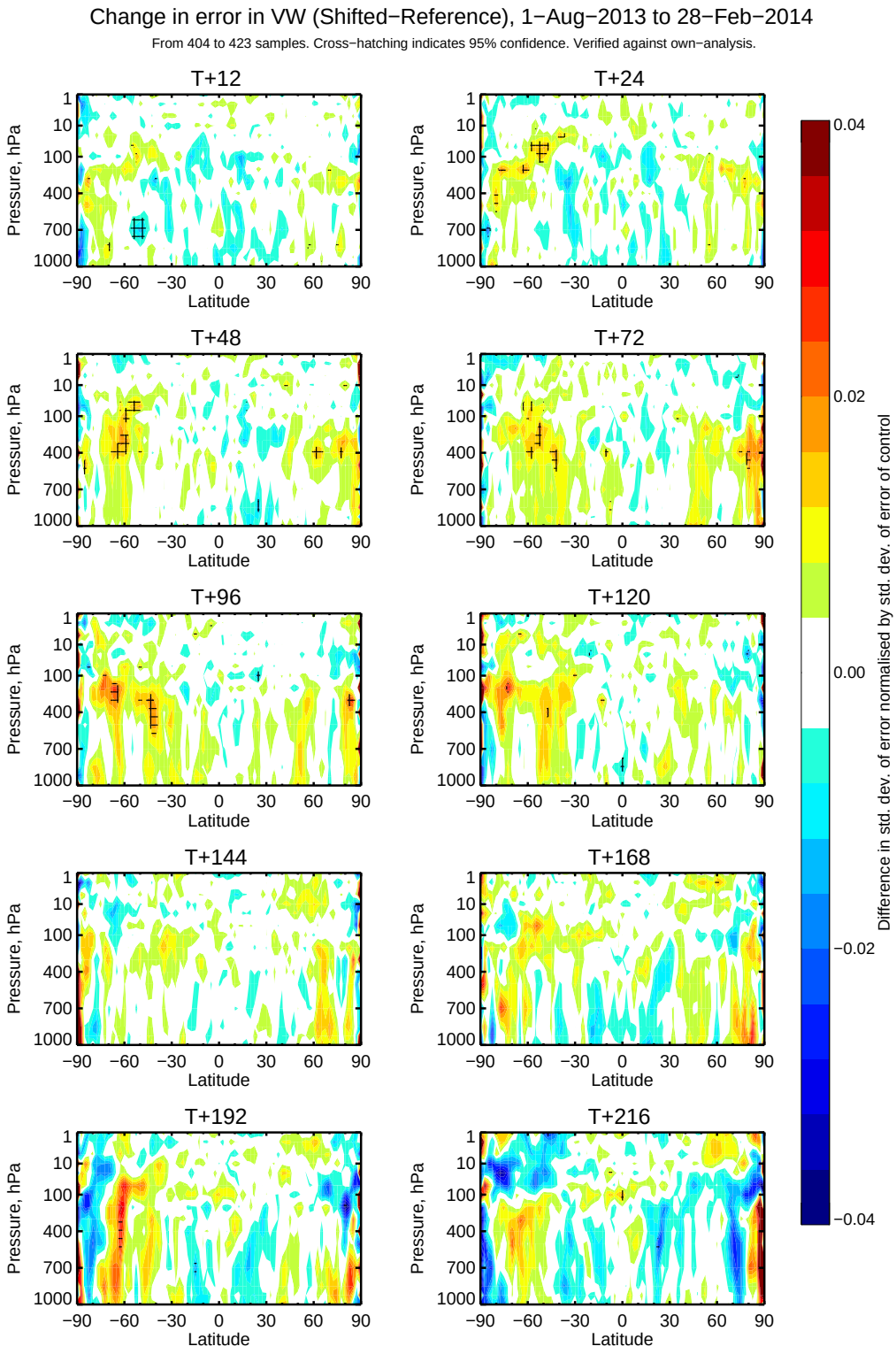

Figure 25: Same as Figure 24 but, between the 'Shifted run' and the 'Reference run'.

5 Conclusions

AMSU-A observations are used widely in NWP models and have important contributions to today's forecast skill. Understanding the physical causes of systematic biases in AMSU-A channels near 60 GHz is an important step in enhancing the data assimilation system.

Two physically-motivated approaches were used in this study to deal with the AMSU-A biases within ECMWF's Integrated Forecasting System. Both approaches assume that the biases originate from the radiative transfer modelling: the first one uses empirical gamma-corrections that scale the optical depth, without attempting to explicitly model the precise mechanism behind the need for scaling, whereas the second one uses modified channel centre frequencies, assuming that the observed biases are solely due to shifts in the channel passbands. Experiments were performed here to evaluate and possibly update in the IFS the AMSU-A coefficient files correcting for air mass dependent biases in AMSU-A observations by either of two physically-based approaches.

When AMSU-A channels 5 to 8 are simulated using either revised γ-corrections or corrected channel central frequencies (passband shifts), there are generally clear improvements in the fit between model and observations in these channels beyond what can be achieved by VarBC bias correction alone. However, these improvements do not translate into medium-range forecast score improvements, but rather some slight degradations.

The passband shifts give generally less improvement in fits to AMSU-A channels 6 – 8 than the γ-corrections, and they cause a greater degradation in fits to independent data (for example AMSU-A channels 9 and upwards, ATMS, radiosondes and satellite winds), particularly in the lower stratosphere and parts of the troposphere. A passband shift does not just move the weighting function up in the atmosphere but it also broadens it, giving an enhanced sensitivity in the lower stratosphere at levels up to 20 hPa. If the short-range lower stratospheric forecast is degraded, it suggests that this additional lower-stratospheric sensitivity is incorrect. Further, it is clear from Figure 18 that the airmass-dependent bias pattern encountered in channels 7 and 8 are also found in channels 9 and 10, albeit with smaller amplitude. As the local oscillator for the latter channels is phase-locked and hence should not be affected by passband shift, the presence of such biases points to a different source, for instance forecast model bias, which may at least partially contribute to the biases observed in channels 7 and 8 as well. Hence, our work does not fully support the 10 MHz to 38 MHz passband shifts that have been empirically diagnosed for channels 6 – 8 on every AMSU-A. However, this does not rule out passband shift as a plausible mechanism for some of the biases in some channels, particularly for NOAA-15 channel 6 and NOAA-16 channels 6 to 8, for which the diagnosed passband shifts appear to drift over time (Zou and Wang, 2011; Lu and Bell, 2014), therefore firmly pointing to an instrument-related issue. Nevertheless, it is likely that part of the total bias for all channels has another physical explanation, and that this bias has been incorrectly aliased into the passband-shift estimates.

The γ-corrections generally do the best in terms of fits to AMSU-A channels 6 – 8 and unlike the passband shifts they do not degrade the short-range forecasts in the lower stratosphere for independent observations. This supports a radiative transfer modelling error as the physical explanation for the air-mass dependent bias that affects all AMSU-As, one that simulates Jacobians (or weighting functions) that are slightly too low in the atmosphere. Spectroscopic errors are one plausible explanation for the bias modelled by the γ-corrections (for example errors in modelling the oxygen lines or continuum). Lu *et al.* (2011) did not see much effect from 2% to 5% perturbations of line strength or width. More recently, Makarov *et al.* (2013) compared a new model for the line mixing effect in the 60 GHz atmospheric oxygen band to the widely used model of Liebe *et al.* (1992) that is used by RTTOV. Significant differences were found. This suggests that the representation of line mixing may also be a significant source of error

in radiation propagation models. Any spectroscopic error would have to be equivalent to an increase in optical depths of around 2%. If we believe that the underlying cause is the same (i.e., spectroscopic errors), then it would be sensible to use the same γ-corrections for all satellites. However, γ also models some aspects of passband characteristics, and it could, for instance, address deviations of the actual passband shapes from the idealised rectangular functions assumed in the radiative transfer calculations. This aspect may well be partially satellite-dependent. It would be highly beneficial if for future missions the detailed spectral response functions were made available to the user community. This has been common practice with infrared instruments for decades.

The degradations shown in medium-range forecast scores for both physically-motivated corrections nevertheless suggest that there may be some deficiencies in the empirically-derived corrections. One additional possibility is that the air-mass dependent error is explained by forecast model bias and this bias may have been aliased incorrectly into the γ- or passband shift estimates. For example if the lower stratosphere were too cool in midlatitudes this could generate similar air-mass dependent biases. These could be generated by excess leakage of humidity from the troposphere to the stratosphere, causing excessive radiative cooling, and such biases could affect any forecast model. Removing these model biases through static γ-corrections or passband shifts would remove the ability of AMSU-A to contribute to recognising and correcting these structures. The attribution and separation of biases arising from different sources is still a challenge and recently projects such as GAIA-CLIM (Gap Analysis for Integrated Atmospheric ECV Essential Climate Variable - Climate Monitoring) are attempting to provide a more accurate assessment of systematic biases in observations.

There are difficulties in using fixed corrections in the form of coefficient tables for biases that may be changing with time (e.g. NOAA-16 channels 7 and 8) and where new satellites are being added (e.g. bandpass corrections for Metop-B were not available for this work). The physically-based corrections need to be derived offline and updated at suitable intervals. In practice this is a lot of work and operational corrections will inevitably end up being out of date. This gives support for using VarBC to correct these biases. In our tests we did have reasonably up-to-date corrections (derived between 2011 and 2013, depending on the method, and applied in 2013). To check if such issues have affected the results of this work, we have also re-run the passband shift experimentation with NOAA-16 AMSU-A removed from the system and the conclusions are unaffected.

In summary, our results do not support the operational use of the modified AMSU-A coefficient files using analysed passband shifts estimated by Lu and Bell (2014). The γ-correction approach corrects air-mass dependent biases for the majority of AMSU-A instruments and although the γ-corrections does not enable us to discriminate between forecast model, instrument or spectroscopic errors, it is in this study found to model departure biases reasonably well. Nevertheless, VarBC on its own can be used to correct the air-mass dependent AMSU-A biases from whatever source and in terms of the quality of forecasts, the VarBC approach is currently best.

Acknowledgements

The first author acknowledges the funding provided through the EUMETSAT NWP-SAF programme. Review comments from William Bell (Met Office) are greatly appreciated.

References

Auligné, T., A. P. McNally and D. P. Dee, 2007: Adaptive bias correction for satellite data in a numerical weather prediction system. *Q. J. R. Meteorol. Soc.*, **133**, 631-642.

Bormann, N. and P. Bauer, 2010: Estimates of spatial and inter-channel observation error characteristics for current sounder radiances for NWP, part I: Methods and application to ATOVS data. *Q. J. R. Meteorol. Soc.*, **136**, 1036-1050.

Bormann, N., A. Geer and T. Wilhelmsson, 2011: Operational implementation of RTTOV-10 in the IFS. *ECMWF Tech. Memo.*, **650**, ECMWF, Reading, UK.

Bormann, N., A. Fouilloux and W. Bell, 2013: Evaluation and assimilation of ATMS data in the ECMWF system, *J. Geophys. Res. Atmos.*, **118**, 12970-12980.

Bormann, N., 2014: Reformulation of the emissivity Kalman Filter atlas, *ECMWF RD Memorandum*, RD14-190, ECMWF, Reading, UK.

Cardinali, C., 2009: Monitoring the observation impact on the short-range forecasts. *Q. J. R. Meteor. Soc.*, **135**, 239-250.

Dee, D., 2005: Bias and data assimilation. *Q. J. R. Meteorol. Soc.*, **131**, 3323-3343.

Di Tomaso, E. and N. Bormann, 2011: Assimilation of ATOVS radiances at ECMWF: first year EUMETSAT fellowship report. *EUMETSAT/ECMWF Report*, **22**, ECMWF, Reading, UK.

Kållberg, P., P. Berrisford, B. Hoskins, A. Simmons, S. Uppala, S. Lamy-Thépaut and R. Hine, 2005: ERA-40 Atlas. *ECMWF re-Analysis project report series*, **19**, ECMWF, Reading, UK.

Harris B. A. and G. Kelly G, 2001: A satellite radiance-bias correction scheme for data assimilation. *Q. J. R. Meteorol. Soc.*, **127**, 1453-1468.

Lawrence, H. and N. Bormann, 2015: Scene-dependent observation errors for the assimilation of AMSU-A. *EUMETSAT/ECMWF Fellowship Programme Research Reports*, **39**, ECMWF, Reading, UK.

Lean, K., W. Bell and Q. Lu, 2014: Radiometric biases in AMSU-A resulting from local oscillator drifts and shifts: Improved radiative transfer modelling and impacts in the Met Office NWP system. In *13th Specialist Meeting on Microwave Radiometry and Remote Sensing of the Environment (MicroRad)*, Pasadena, USA.

Liebe, H., 1989: MPM - an atmospheric millimetre-wave propagation model. *Int. J. Infrared Milli.*, **10**, 631-650.

Liebe, H., P. Rosenkranz and G. Hufford, 1992: Atmospheric 60-GHz oxygen spectrum: New laboratory measurements and line parameters. *J. Quant. Spectrosc. Radiat. Transfer*, **48**, 629-643.

Liebe, H., G. A. Hufford and M. G. Cotton, 1993: Propagation modeling of moist air and suspended water/ice particles at frequencies below 1000 GHz. Atmospheric propagation effects through natural and man-made obscurants for visible to mm-wave radiation, AGARD-CP-542, NATO, 3-13-11.

Lu, Q., W. Bell, P. Bauer, N. Bormann and C. Peubey, 2011: Characterizing the FY-3A microwave temperature sounder using the ECMWF model. *J. Atmos. Oceanic Technol.*, **28**, 1373-1389.

Lu, Q. and W. Bell, 2014: Characterizing Channel Center Frequencies in AMSU-A and MSU Microwave Sounding Instruments. *J. Atmos. Oceanic Technol.*, **31**, 1713-1732.

Lupu C. and A. J. Geer, 2015: Operational implementation of the RTTOV-11 in the IFS, *ECMWF Tech. Memo.*, **748**, ECMWF, Reading, UK.

Lupu, C., A. Geer and N. Bormann, 2015: Revision of the microwave coefficient files in the IFS. *ECMWF Tech. Memo.*, **749**, ECMWF, Reading, UK.

Makarov, D. S., M. Yu Tretyakov and C. Boulet, 2013: Line mixing in the 60-GHz atmospheric oxygen band: Comparison of the MPM and ECS model. *J. of Quant. Spectr. and Radiative Transfer*, **124**, 1-10.

Matricardi, M. and Saunders, R., 1999: Fast Radiative Transfer Model for Simulation of Infrared Atmospheric Sounding Interferometer Radiances, *Appl. Opt.*, **38**, 5679-5691.

Matricardi, M., F. Chevallier, G. Kelly and J.-N. Thépaut, 2004: An improved general fast radiative transfer model for the assimilation of radiance observations. *Q. J. Roy. Meteorol. Soc.*, **130**, 153-173.

Matricardi, M., 2008: The generation of RTTOV regression coefficients for IASI and AIRS using a new profile training set and a new line-by-line database. *ECMWF Tech. Memo.*, **564**, ECMWF, Reading, UK.

McNally, A.P., 2007: The assimilation of uncorrected AMSU-A channel 14 to anchor the VarBC system in the stratosphere. *Research Department Memorandum*, R43.8/AM/0715, ECMWF, Reading, UK.

Peubey, C., and Bell, W., 2014: The influence of frequency shifts in microwave sounder channels on NWP Analyses and Forecasts. *J. Atmos. Oceanic Technol.*, **31**, 788-807.

Peubey, C., W. Bell, P. Bauer and S. D. Michele, 2011: A Study on the Spectral and Radiometric Specifications of a post-EPS Microwave Imaging Mission. *ECMWF Tech. Memo.*, **643**, ECMWF, Reading, UK.

Rabier, F., H. Järvinen, H., E. Klinker, J. F. Mahfouf and A. Simmons, 2000: The ECMWF operational implementation of four-dimensional variational assimi-lation. Part I: experimental results with simplied physics. *Q. J. R. Meteorol. Soc.*, **126**: 1143-1170.

Saunders, R., Matricardi, M. and Brunel, P., 1999: An improved fast radiative transfer model for assimilation of satellite radiance observations. *Q. J. R. Meteorol. Soc.*, **125**, 1407-1425.

Watts, P. and A.P. McNally, 2004: Identification and correction of radiative transfer modelling errors for atmospheric sounders: AIRS and AMSU-A. In *Proceedings of the ECMWF Workshop on Assimilation of High Spectral Resolution Sounders in NWP.* ECMWF, Reading, UK.

Saunders R., J. Hocking, D. Rundle, P. Rayer, M. Matricardi, A. Geer, C. Lupu, P. Brunel, J. Vidot, 2013: RTTOV-11: Science and validation report. *NWP-SAF report*, Met.Office, UK.

Tretyakov, M. Yu., M. A. Koshelev, V. V. Dorovskikh, D. S. Makarov and P. W. Rosenkranz 2005: 60-GHz oxygen band: precise broadening and central frequencies of fine-structure lines, absolute absorption profile at atmospheric pressure, and revision of mixing coefficients. *J. Molecular Spectroscopy*, **231**, 1-14.

Zou, C.-Z. and W. Wang, 2011: Intersatellite calibration of AMSU-A observations for weather and climate applications. *J. Geophys. Res.*, **116**, D23113.